Tumor-associated NK cells drive MDSC-mediated tumor immune tolerance through the IL-6/STAT3 Axis

Shi-Yong Neo[1,2,14], Le Tong[1], Joni Chong[2], Yaxuan Liu[1], Xu Jing[3], Mariana MS Oliveira[3], Yi Chen[1,4], Ziqing Chen[1,5], Keene Lee[2], Nutsa Burduli[6], Xinsong Chen[1], Juan Gao[3,7], Ran Ma[1,8], Jia-Pei Lim[1], Jianxin Huo[2], Shengli Xu[2,9], Evren Alici[6], Stina L Wickström[1], Felix Haglund[1,10], Johan Hartman[1,10], Arnika K Wagner[6], Yihai Cao[3], Rolf Kiessling[1,11], Kong-Peng Lam [2,12,13], Lisa S Westerberg[3], Andreas Lundqvist[1]

[1]Department of Oncology-Pathology, Karolinska Institutet, 17164 Stockholm, Sweden

[2]Singapore Immunology Network, Agency for Science, Technology and Research, Singapore 138648, Republic of Singapore

[3]Department of Microbiology, Tumor and Cell biology, Karolinska Institutet, 17165 Stockholm, Sweden

[4]Department of Medicine, Division of Hematology and Oncology, Columbia University Irving Medical Centre, New York, NY10032, USA

[5]Department of Molecular Biology, Lewis Thomas Laboratory, Princeton University, Princeton, New Jersey, NJ 08540, USA

[6]Department of Medicine Huddinge, Karolinska Institutet, 14152 Stockholm, Sweden

[7]Department of Infectious Diseases, The Third Affiliated Hospital, Sun Yat-sen University, Guangzhou, China 510631, China

[8]Department of Technical Operations, Cepheid AB, Stockholm 17154, Sweden.

[9]Department of Physiology, Yong Loo Lin School of Medicine, National University of Singapore, Singapore 119228, Republic of Singapore

Commented [DH1]: Journal style avoids the use of the word "via"; please change to "through", "by", or similar.

Commented [SYN2R1]: ok

Commented [DH3]: Please include zipcodes for all affiliations

Commented [NSY4R3]: ok

[10]Department of Clinical Pathology and Cancer Diagnostics, Karolinska University Hospital, 17176 Stockholm, Sweden

[11]Theme Cancer, Patient area Head and Neck, Lung and Skin Cancer, Karolinska University Hospital, 17177 Stockholm, Sweden

[12]Department of Microbiology & Immunology, Yong Loo Lin School of Medicine, National University of Singapore, Singapore 119228, Republic of Singapore

[13]School of Biological Sciences, Nanyang Technological University, Singapore 637551, Republic of Singapore

[14]Corresponding author shiyong.neo@ki.se

Single sentence summary: Tumor-associated NK cells induce myeloid-derived suppressor cells to suppress anti-tumor T cell responses

Abstract

Apart from their killer identity, natural killer (NK) cells have integral roles in shaping the tumor microenvironment. Through immune gene deconvolution, the present study revealed an interplay between NK cells and myeloid-derived suppressor cells (MDSCs) in non-responders of immune checkpoint therapy. Given that the mechanisms governing the outcome of NK-myeloid cell interactions remain largely unknown, we sought to investigate the crosstalk between NK cells and suppressive myeloid cells. Upon contact with tumor-experienced NK cells, monocytes and neutrophils displayed increased expression of MDSC-related suppressive factors along with increased capacities to suppress T cells. These changes were accompanied by impaired antigen presentation by monocytes and increased ER stress response by neutrophils. In a cohort of patients with sarcoma and breast cancer, the production of IL-6 by tumor-infiltrating NK cells correlated with S100A8/9 and Arginase-1 expression by MDSCs. At the same time, NK cell-derived IL-6 was associated with tumors with higher major histocompatibility complex (MHC) class I expression which we further validated with *b2m*-KO tumor mice models. Similarly in syngeneic WT and *IL-6* KO mice models, we then demonstrated that the accumulation of MDSCs was influenced by the presence of such regulatory NK cells. Inhibition of the IL6/STAT3 axis alleviated suppression of T cell responses, resulting in reduced tumor growth and metastatic dissemination. Taken together, these results characterize a critical NK cell-mediated mechanism that drives the development of MDSCs during tumor immune escape.

Commented [DH5]: This needs to be no longer than 250 words, this is currently a bit short and more details on mechanism and methods can be included

Commented [NSY6R5]: Ok. Current word count:230.

Commented [DH7]: Since this nomenclature is used throughout is this an official term or would tumor-exposed make more sense, since we have a broad audience this would to make it more accessible for readers, but if this a technical term used in the field please ignore this suggestion

Commented [NSY8R7]: We prefer tumor-experienced

Commented [DH9]: Please include this was done in mice

Commented [SYN10R9]: rephrased to provide more details

Introduction

Throughout the years, mechanisms of tumor immune escape have been extensively studied to improve the success of cancer immunotherapy. In several studies, and across different types of cancer, accumulation of CD8 T cells within the tumor microenvironment (TME) is a key determinant of responsiveness to immune checkpoint inhibition (*1*, *2*). Tumor progression per se is commonly associated with immune tolerance accompanied by the accumulation of immunosuppressive immature myeloid cells (*3*, *4*). These are referred to as myeloid-derived suppressor cells (MDSCs), which suppress anti-tumor CD8 T cell responses across several different cancers (*5*-*8*). For instance, in breast cancer, tumor progression is associated with the expansion of MDSCs in the bone marrow, and their depletion results in reduced tumor progression (*9*). As recently reviewed, the biology of MDSCs is still elusive taking into consideration its versatile adaptation to different pathological contexts (*10*).

The main function of NK cells is to surveil and eradicate virus-infected and transformed cells. However, the plasticity of NK cell functions and phenotypes depend on the context and location where the cells reside. NK cells are known to produce several cytokines such as GM-CSF, and IL-10 (*11*-*14*), potentially influencing the fate of myeloid cell differentiation within the TME (*15*-*18*). Although the effect of myeloid cells on NK cell functions has been widely studied, less is known of how NK cells influence the function of myeloid cells during this bi-directional intercellular interplay (*19*-*24*). A recent study demonstrated that NK cells influence the differentiation of dendritic cells (DC) by downregulation of HLA-DR in non-small cell lung cancer (NSCLC) (*25*). However, how NK cells drive the development of MDSCs is not clear.

Commented [DH11]: Please spell out all acronyms and gene names at first instance.

Commented [NSY12R11]: ok

Commented [DH13]: Author ok? I think how it was previously was a bit confusing

Commented [SYN14R13]: ok

Our present study reports a unique inflammatory gene signature that correlated with higher NK cell abundance in non-responders to immune checkpoint blockade. Upon tumor exposure in vitro, NK cells acquired a regulatory phenotype to induce MDSCs derived from both monocytes and neutrophils through the IL-6/STAT3 axis. Moreover as demonstrated in vitro co-cultures, tumor-associated NK cells enhanced the ER stress responses of neutrophils, sustaining their capacity to inhibit CD8 T cell responses. We demonstrate that NK cells disrupt the antigen presentation by monocytes to impact tumor recognition by tumor-infiltrating lymphocytes (TILs). Our findings identify a non-canonical mechanism in which tumor-associated NK cells display an influential role in MDSC-mediated immune suppression in the TME.

Commented [DH15]: In vitro?

Commented [SYN16R15]: yes

Commented [DH17]: Again in what model?

Commented [SYN18R17]: amended to provide better clarity

Results

A unique Inflammatory gene signature correlates with an NK cell signature in non-responders to immune checkpoint blockade

To date, many transcriptomics studies have been performed on patient cohorts receiving treatment with immune checkpoint inhibitors (ICIs). Yet, there is a paucity of factors to coherently predict responsiveness to therapy. An early study reported an immune suppressive gene signature characterized by a set of upregulated inflammatory genes and downregulated genes for antigen presentation and adaptive response (*26*). Based on this gene expression profile, we devised an alternative inflammatory gene signature by filtering for immune-related genes from the upregulated gene set (table S1).

Batch-correcting a pool of three distinct patient cohorts undergoing anti-PD-1/PD-L1 (Programmed cell death protein-1/Programmed death-ligand 1) therapy for gene expression analysis, we observed a general trend that genes within the inflammatory signature were increasingly expressed in patients with higher scores of an established NK gene signature (*27*) (Fig. 1A and Fig. S1A). Next, we evaluated if there was a correlation between the inflammatory and NK signature scores with clinical outcomes within the three individual cohorts. In the first cohort of patients with esophageal cancer in which samples were collected pre- and on-treatment with atezolizumab (GSE165252), the inflammatory gene expression score was increased (P=0.0313 in responders, P=0.0046 in non-responders) upon treatment in a within-subjects comparison (Fig. S1B). Only in the non-responder group, a correlation between inflammatory and NK cell scores in both baseline samples and on-treatment samples was observed. A higher greater correlation of NK and inflammatory scores were observed in on-treatment samples as compared with baseline samples (Fig. 1B and 1C). Similarly, in the next cohort of patients with melanoma and receiving pembrolizumab

Commented [DH19]: Please verify and bring to our attention if the following applies:1. any reagents or materials are not publicly available and will require an MTA to be provided to readers 2. Any large datasets that require public deposition - include the accession number (this includes genomics, transcriptomics, proteomics etc.) code used to process this data is required to be publicly available as well on Zenodo 3. If you have funding from a Plan S funder and require open access after publication

Commented [SYN20R19]: understood

Commented [DH21]: For experiments with n < 20, we ask that data be reported in tabular format. This is most easily accomplished with a separate Excel file with data from figures organized on separate tabs. See Checklist

Commented [NSY22R21]: Ok noted

Commented [DH23]: For tables please use lowercase “t”, for the supplemental tables use table S# and for main tables just table #

Commented [SYN24R23]: ok

Commented [DH25]: Please spell out at first use

Commented [NSY26R25]: ok

Commented [DH27]: Author, correct?

Commented [SYN28R27]: correct

Commented [DH29]: Main figures are presented as Fig. #, supplementary as fig. S#. (e.g., Fig. 1, fig. S1).

Commented [SYN30R29]: noted. will amend throughout

Commented [DH31]: Please present results in past tense

Commented [NSY32R31]: noted

Commented [DH33]: As per our style, we prefer the form 'patients with cancer' instead of 'cancer patients' in order to avoid identification of the subjects with the disease.

Commented [SYN34R33]: ok

Commented [DH35]: Is this statistically significant, if yes please include P-value

Commented [SN36R35]: ok

treatment (GSE78220), a stronger positive correlation of NK and inflammatory scores in non-responders as compared with responders to treatment was observed (Fig. 1D). Further substantiating our observations, the third cohort of mixed tumors (GSE93157) was analyzed in which patient responses to anti-PD-1 therapy were classified based on the RECIST criteria. A positive correlation between NK and inflammatory gene signatures was observed only in the progressive disease (PD) group and not in the stable disease (SD) or the complete/partial response group (CR/PR) (Fig. 1E). Using the ssGSEA(Single-sample gene set enrichment analysis) algorithm, the NK cell gene signature used herein showed a strong correlation (P<0.0001) with two other reported NK cell gene signatures in all three respective patient cohorts, indicating that our findings were not limited to a specific NK cell signature (Fig. S1C to 1E) (*28*, *29*).

To further substantiate the role of NK cells in non-responders of immune checkpoint blockade, we analyzed a publicly available single cell transcriptomic dataset in which a cohort of patients with breast cancer were grouped based on T cell expansion in response to anti-PD1 therapy (*30*). Within the originally defined myeloid population, unsupervised clustering to further profile various macrophages and monocytic subsets was performed. A subset of CD68 negative myeloid cells that co-express S100A8 and S100A9 (cluster 6) was identified (Fig. 1F). Within the NK cell population, we identified three clusters (NK1, NK2 and NK3) (Fig. S1F). Several correlations between NK and CD68$^{low/neg}$ myeloid subsets were observed only in patients with no T cell expansion (Fig. 1G and H). In comparing these three clusters, the NK1 cluster correlated with increased myeloid abundance and also showed high CD69 and NKG2A, and low granzyme B, perforin, and CD16 expression (Fig. S1F). Taken together, these observations highlight the clinical relevance to further investigate the

Commented [DH37]: Please spell out at first use

Commented [SYN38R37]: ok

Commented [DH39]: Is this significant? See prior comment

Commented [SYN40R39]: p value can be included here

Commented [DH41]: As per our style, we prefer the form 'patients with cancer' instead of 'cancer patients' in order to avoid identification of the subjects with the disease.

Commented [SYN42R41]: amended

Commented [DH43]: How many clusters, please define this at first use

Commented [SYN44R43]: this is defined in line 78-79.

mechanisms and cell types underlying this correlation between NK cells and inflammation in the context of tumor immune escape.

Tumor-experienced NK cells acquire a distinct CD69+, Perforin- phenotype with immune regulatory functions

Since NK cells with regulatory features have been reported to reside in both tumor and non-tumor tissues (*13, 31*), we sought to first determine if NK cells experience distinct phenotypic changes upon exposure to tumor or non-tumor cells. By spectral flow cytometry, we defined subsets of NK cells based on maturity and observed a distinct upregulation of CD69 and downregulation of Perforin in tumor-experienced NK cells as compared to unstimulated control or NK cells exposed to non-tumor HepaRG cells (Fig. 2A and B). Downregulation of CD16 was observed together with transcriptional regulators such as EOMES and IKAROS in these co-cultured NK cells (Fig. 2C). Using the same co-culture conditions, FACS-sorted NK cells were analyzed by RNA sequencing to uncover transcriptional reprogramming concomitant with the observed immune suppression. Pathway enrichment analysis revealed that genes differentially upregulated in tumor-experienced NK cells were associated with genesets regulating immune activation and differentiation (Fig. 2D). Genes upregulated included inflammatory cytokines such as *EBI3* (IL-35), *TNF*, *IFNG* and *CSF2* (Fig. S2A to C). Additionally, when compared to control NK cells, tumor-experienced NK cells also expressed higher amounts of *CD274* and *TNFRSF9* (encodes for PD-L1 and 4-1BB respectively) which was previously reported in CD73 positive immune regulatory NK cells (*13*) (Fig. S2C). Given that we previously reported that CD69+ NK cells and monocytic MDSCs predict worse prognosis in an advanced melanoma cohort receiving anti-PD1 treatment (*32*), the present study highlights that CD69 is also upregulated in tumor-

experienced NK cells, suggesting that CD69 denotes NK cells with regulatory roles within the tumor microenvironment.

Tumor-experienced NK cells induce suppressive monocytes with defective antigen presentation to CD8 T cells

To investigate whether tumor-experienced NK cells influence the phenotype and function of myeloid cells, NK cells were either pre-cultured with patient-derived tumor cell lines (tumor-experienced) or not (control NK cells) and thereafter purified and co-cultured with autologous monocytes. Compared to monocytes alone, an increase in the expression of HLA-DR was observed upon co-culture with control NK cells. In contrast, compared to monocytes co-cultured with control NK cells, a decrease in HLA-DR expression was observed in monocytes upon co-culture with tumor-experienced NK cells (Fig. 3A). When monocytes were cultured with NK cells pre-cultured with non-tumor cells, an increase in HLA-DR expression was observed (Fig. S3A and 3B). Upon co-culture with tumor-experienced NK cells, monocytes upregulate CD73 (P=0.0417), arginase-1 (ARG-1) (P=0.0475) and PD-L1 (P=0.0004) as compared to monocytes cultured alone (Fig. 3B to D). On the other hand, PD-L1 was not upregulated on monocytes cultured with NK cells pre-cultured with non-tumor cells (Fig. S3C). Similar to tumor-experienced NK cells, tumor-supernatant cultured NK cells reduced HLA-DR expression on myeloid cells (Fig. S3D). Compared with monocytes cultured with tumor-experienced NK cells, the frequencies of CD163/CD206 double negative and double positive monocyte populations were lower and higher when cultured with tumor supernatant NK cells respectively (Fig. S3E and 3F).

Given that the downregulation of HLA-DR is characteristic of monocytic-MDSC (M-MDSC) phenotype (*33*), the suppressive capacity of FACS-sorted HLA-DR^{low} NK cell experienced

monocytes was evaluated (Fig. S3G). The proliferation of autologous CD8 T cells was only suppressed by monocytes pre-cultured with tumor-experienced NK cells (Fig. 3E and 3F). To test if these suppressive factors were responsible for the inhibition of T cell proliferation, selective inhibitors were added to T cell suppression assays. Whereas inhibition of CD73 and ARG-1 (NOHA treatment) did not rescue T cell proliferation, the inhibition of PD-L1 (Atezolizumab) alleviated the suppression of T cell proliferation (Fig. 3G and S3H).

Commented [DH45]: There is no Fig 2H do you mean 3G?

Commented [SYN46R45]: amended

Since MDSCs display defective antigen presentation capacity (*7*, *34*), an HLA-A2 matched co-culture of NK cell-induced myeloid cells with patient-derived Tumor-infiltrating lymphocytes (TILs) was designed to test the antigen presentation in the presence of tumor lysates or previously identified neo-epitopes (*35*) (Fig. 3H). Antigen-loaded monocytes alone and monocytes pre-cultured with control NK cells stimulated TILs to produce IFNγ upon re-stimulation with autologous tumor cells. In contrast, the production of IFNγ by TILs was dampened when co-cultured with antigen-loaded monocytes pre-conditioned with tumor-experienced NK cells (Fig. 3I). Only a minimal IFNγ response (non-significant) was observed upon exposure to autologous tumor cells when TILs were cultured with monocytes not loaded with antigens, thereby excluding any potential alloreactive effect due to healthy donor monocyte stimulation of patient-derived TILs (Fig. S3I). Collectively, these results show that upon tumor contact, NK cells acquire regulatory functions to potentiate immunosuppression and dampen the antigen presentation by monocytes.

Commented [DH47]: Please spell out at first use

Commented [SYN48R47]: ok

Commented [DH49]: Non-significant?

Commented [SYN50R49]: yes. non significant

Tumor-experienced NK cells enhance survival and proliferation of sXBP1+ suppressive neutrophils

To explore whether tumor-experienced NK cells also affect the immune biology of neutrophils, NK cell-neutrophil co-cultures and suppression assays were performed (Fig. 4A).

Since the viability of neutrophils can be compromised ex vivo, neutrophils were stained for active caspase-3/7 in the presence or absence of NK cells. Whereas increased viability of neutrophils was observed in the presence of tumor-experienced NK cells compared to neutrophils cultured without NK cells (p=0.006), control NK cells did not influence the viability of neutrophils (Fig. 4B and 4C). In terms of suppressive factors associated with polymorphonuclear (PMN)-MDSCs, both control and tumor-experienced NK cells induced the upregulation of COX-2 (Fig. 4D and E). Furthermore, control and tumor-experienced NK cells induced arginase-1 (ARG-1) expression in neutrophils, but only when cultured with tumor-experienced NK cells did the frequency of ARG-1 positive neutrophils significantly increase (Fig. 4D and F). Although neutrophils cultured with tumor-experienced NK cells had similar amounts of ROS accumulation as compared to neutrophils alone, neutrophils co-cultured with control NK cells showed lower amounts of ROS in contrast to when cultured with tumor-experienced NK cells (Fig S4A). Compared with control NK cells, under the influence of tumor-experienced NK cells, neutrophils acquired the ability to suppress CD8 T cell activation, as measured by the production of IFNγ and expression of the activation marker CD69 (Fig. 4G and S4B).

One of the recently established concepts to distinguish PMN-MDSCs from neutrophils is the activation of ER stress, implicating altered cell function and survival within the TME (*36*, *37*). Although neutrophils showed higher expression of the ER stress response transcription factor spliced XBP-1 (sXBP-1) upon culture with control and tumor-experienced NK cells, only when cultured with tumor-experienced NK cell, neutrophils expressed higher amounts of sXBP-1(Fig. 4H and 4I). Furthermore, the presence of tumor-experienced NK cells induced the upregulation of the Ki67 proliferation marker, particularly in neutrophils expressing sXBP-1 (Fig. 4J). Using tunicamycin to induce ER stress, the viability of

Commented [DH51]: Our style does not italicize in vitro, in vivo, ex vivo, etc. please change throughout

Commented [SYN52R51]: ok

Commented [DH53]: Please include significance

Commented [NSY54R53]: included

neutrophils was maintained (>60%) under increasing ER stress induction only in the presence of tumor-experienced NK cells (Fig S4C). Given that ER stress is associated with suppressive myeloid phenotypes, tunicamycin pre-treatment further enhanced suppression of T cell activity by neutrophils only in the presence of tumor-experienced NK cells (Fig. 4K). Through these series of experiments, we demonstrate how the suppressive capabilities of neutrophils depend on the presence of tumor-experienced NK cells during ER stress.

Combinatorial analysis of NK cells and MDSCs within patient tumors reveals NK cell-derived IL-6 as a driver for suppressive myeloid phenotypes

To substantiate our in vitro findings, phenotyping of tumor-infiltrating NK cells and myeloid cells was performed in treatment-naïve tumor resections from patients with breast cancer and sarcoma (Patient characteristics in tables S2 and S3). We first validated the abundance of NK cells in both breast cancer and sarcoma primary tumors (Fig. 5A and S5A). In the breast cancer cohort, higher frequencies of NK cells correlated with higher proportions of CD15+ granulocytes and reduced frequencies of CD11c+, HLA-DR^{high} myeloid cells. At the same time, frequencies of NK cells negatively correlated with total CD3+ T cells and PD-1+ CD8 T cells (Fig. 5B). In the sarcoma cohort, frequencies of NK cells positively correlated with HLA-DR^{low} CD14+ cells (Fig. S5B). From repository-accessed flow cytometry data (*38*), NK cells also negatively correlated with PD-1+ CD8 T cells and total T cells, and concurrently correlated with either HLA-DR^{low} or PD-L1+ CD68 myeloid cells in colorectal cancer (CRC) and glioblastomas (GBM). However, these correlations were not observed in lung cancer (NSCLC) and renal cancer (RCC) (Fig. S5C).

With further flow cytometric analysis, cytokines specifically produced by NK cells were studied in relation to various suppressive myeloid cell markers from sarcoma and breast

Commented [DH55]: Were these pre or post therapy?

Commented [SYN56R55]: treatment naive samples

cancer tumor samples. Within the sarcoma cohort, tumor-infiltrating NK cells produced GM-CSF, IL-4, IL-6, IL-10, IFNγ and TNF (Fig. S5D). Subsequent analysis revealed that NK cell-derived IL-6 correlated with the expression of S100A8/9 and arginase in CD14+ M-MDSCs, and that NK cell-derived IL-10 negatively correlated with the frequency of CD11c+, HLA-DR^{high} myeloid cells (Fig. S5E). In contrast to these findings, no significant correlation was observed between arginase and S100A8/9 with any of the cytokines produced by T cells. Instead, a positive correlation between T cell-derived GM-CSF and arginase-positive M-MDSCs was observed (Fig. S5F). We next investigated whether NK cells within breast cancers similarly produce IL-6. Across various cell types within breast tumors, we identified both CD14+ myeloid cells and NK cells to be the higher sources of IL-6 in contrast to T cells and non-immune cells (Fig.5C).Although it has already been established that tumors drive myeloid cells into immune-suppressive phenotypes, our findings suggest a previously unidentified mechanism whereby tumor-infiltrating NK cells acquire regulatory properties to induce MDSCs within the tumor immune landscape.

Commented [DH57]: Author, correct?

Commented [SYN58R57]: correct

Tumor MHC class I expression influences NK cell-derived IL-6 and frequency of myeloid cells

Given that MHC class I (MHCI) expression greatly influences NK cell responses and that inflammation and the global downregulation of MHC class I reset NK cell education to regulate its function (*39*), we next sought to investigate the likelihood of tumor MHCI expression influencing NK cell production of IL-6 and the abundance of MDSCs. In the breast cancer cohort, an association of S100A8/9+ M-MDSCs and IL-6 producing NK cells was observed in tumors with high MHCI expression (Fig. 5D and E). In vivo after 14 days post inoculation of B16F10 tumor cells, we validated that the frequency of NK cells producing IL-6 or IL-10 was higher in wild type (WT) tumors than in *b2m*-KO B16F10

tumors lacking MHCI expression (Fig. 5F). At the same time, B16F10 tumors contained higher frequencies of M-MDSC (*P*=0.0002) and PMN-MDSC (*P*=0.0169) when compared with *b2m*-KO tumors (Fig. 5G and 5H). In a separate in vivo B16F10 experiment, depletion of NK cells resulted in reduced frequencies of M-MDSC but not PMN-MDSC (Fig. 5I). Similarly at 14 days post tumor inoculation, the depletion of NK cells resulted in lower frequencies of M-MDSC in RMA tumors but not in RMA-S (TAP2-deficient variant) tumors in C57BL/6 WT mice (Fig. 5J). A higher frequency of IL-6 producing NK cells was observed in RMA tumors as compared with RMA-S tumors (Fig. 5K and 5L). On the other hand, the frequency of PMN-MDSC was not altered in mice bearing RMA and RMA-S tumors (p=0.17) or upon NK cell depletion (p=0.21), suggesting that the PMN-MDSC response may be regulated by alternative tumor factors in vivo.

Given the potential influence of NK cells to regulate MDSC frequencies, we next sought to investigate the potential relationship between NK cells and tumor-associated macrophages (TAMs). Similar to the frequency of MDSCs, the frequency of macrophages was reduced in NK cell-depleted B16F10-bearing mice (Fig. S6A). Unlike what was observed in frequencies of MDSCs, no significant difference was observed in the frequency of macrophages between wildtype (WT) B16F10 and *b2m*-KO B16F10 tumors (Fig. S6B). Unlike B16F10 tumors, which had lower basal expression of MHC class I, RMA tumors had decreased frequencies of TAMs compared with MHC class I-deficient RMA-S tumors, and depletion of NK cells increased the frequency of TAMs in RMA-S tumors (Fig. S6D). In addition, RMA-S tumors showed an increased frequency of M1 macrophages compared with RMA tumors, and depletion of NK cells resulted in further increased M1 macrophage frequency in RMA-S tumors (Fig. S6E).

Commented [DH59]: Please include P-value

Commented [NSY60R59]: Ok included

Commented [DH61]: What was the timing relative to tumor inoculation?

Commented [NSY62R61]: Depletion treatment was given on day -1, 6 and 13. We will specify this and the endpoints clearer in methods .

Commented [DH63]: Please include mouse strain

Commented [SYN64R63]: ok

Commented [DH65]: For all of these tumors when were these evaluated, how many days past inoculation or at what size?

Commented [NSY66R65]: 14days. Now added for B16F10 and RMA. Also added in methods.

To further substantiate these findings, MDSC and macrophage frequencies were analyzed in the 4T1 and MC38 tumor models. Similar to results obtained in the B16F10 and RMA models, *b2m*-KO 4T1 breast tumors showed a reduced frequency of M-MDSCs and an increased frequency in total macrophages compared with WT 4T1 tumors (Fig. S6F to G). With regards to the inflammatory state of TAMs, the frequency of M1 macrophages was higher in *b2m*-KO B16F10, RMA-S, and *b2m*-KO 4T1 tumors than in the WT tumors (Fig. S6C, E, H).

In contrast to the B16F10, RMA, and 4T1 models, no significant differences were observed in the frequency of M-MDSCs between WT and *b2m*-KO MC38 tumors. Instead, a reduction of total TAMs in *b2m*-KO MC38 tumors was observed. Consistent with the B16F10, RMA, and 4T1 models, a greater proportion of M1 macrophages was observed in *b2m*-KO MC38 tumors compared with WT tumors (Fig. S7A-C). Taken together, these results show that tumor MHC class I expression and the presence of NK cells influence MDSC and macrophage frequencies in vivo.

NK cell-derived IL-6 increases myeloid iNOS, PD-L1, and arginase expression but does not impact macrophage polarization

To address whether NK cell-derived IL-6 impacts myeloid cells, intratumoral NK cells were isolated from WT or IL-6 KO MC38 tumor-bearing mice and cultured with bone marrow-derived monocytes from naive WT mice. Comparing monocytes cultured with WT NK cells to IL-6 KO NK cells, higher expression of iNOS, PD-L1 and arginase-1 was observed (Fig. 5M). Furthermore, the macrophage marker, F4/80 was upregulated in NK cell-experienced monocytes as compared to the monocyte alone. However, no significant differences in F4/80 and CD206 expression were observed when comparing monocyte cultured with WT NK cells and IL-6 KO NK cells, indicating that NK cell-derived IL-6 is unlikely to have a direct effect on the polarisation of TAM (Fig. S6I). In addition to the observed higher frequency of IL-6

Commented [DH67]: Author, correct?

Commented [NSY68R67]: Amended. Knockouts are the deficient

Commented [DH69]: Author, correct?

Commented [NSY70R69]: correct

positive NK cells in WT MC38 tumors, NK cells in WT MC38 tumors also expressed higher amounts of CD69, TGFβ1 and NKG2A whereasNK cells in B2m-KO tumors expressed higher amounts of NKG2D (Fig. S7D to 7F). In summary, these results support that NK cell-derived IL-6 increase the expression of iNOS, PD-L1, and arginase by myeloid cells, but does not impact on macrophage polarization.

NK cell-derived IL-6 contributes to MDSC-mediated immune suppression and tumor progression

To further evaluate the contribution of IL-6 producing NK cells to promote tumor progression, either isolated WT-NK cells or IL6-KO NK cells were co-injected with B16F10 tumor cells into C57BL/6 WT mice. The growth of B16F10 tumors co-injected with WT NK cells was faster than tumors co-injected with IL6-KO NK cells (Fig. 6A). Although not significant, the final volume of tumors with WT NK cells was slightly larger than tumors without exogenous NK cells injection (Fig. 6B). Subsequent flow cytometry analysis revealed that tumors with WT NK cells had more intratumoral Ly6G+, CD11b+ PMN-MDSCs as compared to tumors without NK cells or with IL6-KO NK cells (Fig. S8A). In addition, reduced numbers of F4/80^{high} intratumoral macrophages were seen in WT NK cells as compared to those with IL6-KO NK cells, even though tumors without exogenous NK cells had similar numbers of these macrophages (Fig. S8B). Moreover, tumors with IL6-KO NK cells showed slightly reduced proportions of PDL1+ intratumoral F4/80^{high} cells compared to tumors with WT NK cells or without NK cells (Fig. S8C).

Next, we sought to determine whether IL-6 production specifically by human NK cells would similarly affect myeloid function and phenotype. Using siRNA, NK cells with impaired IL-6 production were FACS sorted and used in subsequent experiments (Fig. S9A). Compared

Commented [DH71]: Author, correct? And what strain?

Commented [SYN72R71]: amended

Commented [DH73]: Author, correct?

Commented [SYN74R73]: amendment is okay.

with control siRNA, *IL6* siRNA NK cells showed reduced IL-6 production and the ability to induce STAT3 activation in monocytes in vitro (Fig. S9B to 9E). In co-cultures with *IL6* knockdown-NK cells, monocytes expressed lower amounts of multiple MDSC-associated markers such as S100A8/9, Arginase-1, PD-L1, and nitric oxide compared than when co-cultured with NK cells transfected with siRNA scrambled control (Fig. 6C and D). Moreover, CD8 T cell proliferation was inhibited by monocytes primed with IL-6 proficient NK cells compared with monocytes primed with *IL6* knockdown-NK cells (Fig. 6E).

Commented [DH75]: Author, correct?

Commented [SYN76R75]: correct

Commented [DH77]: Do you mean 6E?

Commented [SYN78R77]: amended

Using the zebrafish xenograft model that allows the application of low cell numbers with a large sample size, the contribution of NK cell-derived IL-6 in immune evasion was interrogated. After siRNA incorporation and selection, HLA-A2 matched NK cells were mixed with patient-derived TILs and tumor cells and monitored within the zebrafish larvae (Figure 6F). Compared with zebrafish engrafted with siControl NK cells, a decrease in the number of tumor foci in the whole fish larvae was observed in the presence of *IL6* knockdown-NK cells (Fig. 6G and H). The accumulation of nitric oxide abundance within the zebrafish skeleton has previously been reported (*40*). By using DAF-FM based detection, a reduction in nitric oxide positive regions was observed in the zebrafish injected with *IL6* knockdown-NK cells as compared with si-control NK cells (Fig. 6I). Collectively, these findings further support that NK cell-derived IL-6 contributes to the immune-suppressive effect of myeloid cells and ultimately limits the immune-surveillance capacity of T cells within the TME.

Inhibition of the IL6/STAT3 axis alleviates NK/MDSC-mediated immune suppression of anti-tumor T cell responses

To substantiate our findings from patient samples and syngeneic mouse models, further investigations on the signal transducers commonly associated with myeloid cell functions were performed following co-cultures of NK cells and monocytes (Fig. 7A). Upon co-culture with tumor-experienced NK cells, the activation of phosphorylated STAT3, which is a well-known downstream target of IL-6, was observed in both monocytes and neutrophils (Fig. 7B and 7C).

These observations motivated further exploration to target the IL-6/STAT3 axis in vivo to abrogate NK/MDSC-mediated immune suppression. To block the IL-6/STAT3 axis, the anti-IL-6 receptor antibody Tocilizumab was used in a xenograft setting of adoptive TIL therapy against melanoma. Similar to the IL6-KO NK cell experiments, allogenic NK cells were co-inoculated with primary human melanoma cells (KADA) during the formation of xenograft tumors in NSG mice. On day 7, TILs were injected together with monocytes in the presence or absence of Tocilizumab (Fig. 7D). The presence of NK cells resulted in increased lung metastases (p=0.0209) which were reduced by the addition of Tocilizumab (p=0.0076) (Fig. 7E and 7F). Additional immunohistochemistry staining also revealed these metastasized cells expressed human melan-A (Fig. S10). Furthermore, Tocilizumab treatment reduced the tumor infiltration of human CD14 (huCD14) monocytes (Fig. 7G). The presence of NK cells resulted in higher frequencies of huCD14 monocytes expressing phosphorylated STAT3 within the tumor which was reduced with the administration of Tocilizumab (Fig. 7H). The presence of NK cells was furthermore associated with increased PD-L1 and arginase expression in tumor-infiltrating huCD14 cells. Similar to the alterations of STAT3 activation, the expression of both arginase and PD-L1 on intratumoral huCD14+ monocytes was reduced with tocilizumab treatment (Fig. 7I and 7J). To further validate that the engrafted monocytes had acquired immune-suppressive functions, huCD14+ monocytes were FACS-sorted from

Commented [DH79]: Please include strain and what tumor cells were used

Commented [SN80R79]: Included

Commented [DH81]: Was this significant?

Commented [SN82R81]: P value included in text.

Commented [DH83]: Should this be 7G?

Commented [SYN84R83]: amended

the tumors and tested for their ability to suppress autologous CD8 T cells. Compared with CD8 T cells alone, only monocytes harvested from mice with tumor-infiltrating NK cells without in vivo Tocilizumab treatment showed suppression of CD8 T cell proliferation (Fig. 7K). Taken together, these findings further confirm that the inhibition of the IL-6/STAT3 pathway could alleviate immune suppression and enhance adaptive immune responses, particularly in tumors with high NK cell abundance.

Discussion

The investigation of MDSC is a rapidly advancing research area and recent studies have highlighted their role in tumor progression and response to cancer immunotherapy (*32*, *41-44*). Although the main focus has been to investigate the role of MDSC as inhibitors of T cell immunity, there is an increasing interest to characterize the interaction between MDSC and NK cells (*45*). Earlier studies have explored NK cell-monocyte interactions through similar co-culture experiments, demonstrating a bi-directional activation that drives the production inflammatory cytokines. They found NK cells isolated from inflamed sites were better activators of monocytes as compared to peripheral blood NK cells (*24*). Considering that the mechanism underlying such mutual activation remains elusive, another study demonstrated the role of NKp80-ACIL ligation as a contact-dependent interplay that triggers these inflammatory responses (*23*). However, these studies mainly defined monocyte activation by their ability to produce TNFα and less is known about how NK cells influence myeloid cell development and immune-regulatory functions. Here, we sought to address some of this complexity in the context of tumor immune escape.

Our findings demonstrate how NK cells potentially influence the cellular biology and suppressive functions of both neutrophils and monocytes within the TME. The present study proposes two relevant implications. First, the importance of tumor-infiltrating NK cells should not be neglected even if their abundance may not always correlate with better prognosis in cancer (*46*, *47*). We demonstrate that the influence of tumor-associated NK cells resulted in the failure of monocytes in presenting tumor antigens to TILs, accompanied by the upregulation of MDSC-associated markers such as arginase and S100A8/9. Using zebrafish and murine xenograft models, the presence of NK cells in the tumor even resulted in enhanced tumor migration. Given that a tumor can be resistant to NK cell-mediated

Commented [DH85]: Please make sure to include a paragraph discussing the limitations of your study

Commented [NSY86R85]: noted

cytotoxicity, there is therefore an apparent risk that high NK cell abundance could contribute to the further development of immune tolerance. The second implication relates to the mechanisms underlying the altered cell biology of MDSCs as compared with mature myeloid cells. These mechanisms are not yet fully elucidated and technically challenging to design experimental approaches to address (*10, 48*). Whereas it was demonstrated that PMN-MDSCs activate C/EBP-homologous protein (CHOP) and XBP-1 transcriptional regulators in response to ER stress, there is still a research gap in understanding how these "stressed" MDSCs persist within the TME (*36, 37*). When investigating whether NK cells potentiated the suppressive functions of neutrophils, we did not observe that ER stress was directly related to enhanced suppressive functions of these neutrophils. Rather, our findings suggested that tumor-associated NK cells could aid these XBP-1-positive PMN-MDSCs, reprogramming their cellular fitness to persist and expand in the TME. Future studies should consider studying critical interactions between MDSCs and other cell types within the TME.

Two decades ago, when the concept of MDSCs was not yet established, it was demonstrated that the balance of IL-4 and IL-6 determines the differentiation of DCs to favor anti-tumor immune responses (*49*). Subsequent studies identified several cytokines such as IL-3, IL-6, c-kit ligand, TPO, FLT3L, VEGF, G-CSF, GM-CSF, and M-CSF to potentiate the MDSC phenotype and function (*50-52*). More recently, we found that tumor cells induce the differentiation of MDSCs from monocytes through direct physical contact and through the production of prostaglandin E2 (*53*). NK cells can produce cytokines that favor dendritic cell maturation and function, particularly IL-4, GM-CSF, TNFα and IFNγ (*14*). Moreover, it was demonstrated that NK cell-trained DC are better in priming type 17 CD8 T cells (*19*). A pivotal study by Böttcher et al. demonstrated how NK cells possess a "helper" identity to recruit DCs into the TME (*27*). Clinical investigations have also highlighted the importance

Commented [DH87]: Induce the differentiation of MDSCs from monocytes?

Commented [NSY88R87]: Yes. Amended now.

Commented [DH89]: Journal style avoids the use of the word "via"; please change to "through", "by", or similar.

Commented [SYN90R89]: ok

of dendritic/NK cell interactions concerning the prognosis of patients with neuroblastoma and melanoma (*54*, *55*). Although the focus of this study was to investigate NK cell interaction with MDSCs and macrophages in the context of tumor MHC class I expression, further studies to delineate the influence of tumor MHC class I expression on NK-DC cross talk are needed. On the contrary, several immune-suppressive roles of NK cells were also identified, and therefore, the concept of regulatory NK cells could be highly relevant for understanding the tumor immune biology (*13*, *56*, *57*). From a cohort of patients with advanced melanoma and receiving anti-PD1 therapy, the presence of CD69+ NK cells correlated with a worse overall and progression-free survival (*32*). NK cells that lost their cytotoxic activity were also reported to acquire a pro-metastatic role, contributing to tumor outgrowth (*58*). In breast cancer, higher frequencies of $CD56^{bright}$ NK cells were found to correlate with larger tumor size within tumor tissues (*59*). Moreover, another study also further demonstrated that NK cells support the pro-metastatic role of neutrophils mediated by G-CSF in breast cancer (*60*).

Here, we report correlations of a unique inflammatory gene signature with an NK cell signature in non-responders of several immune checkpoint therapy cohorts. Following up on our previous study, the present work reports a subset of CD69+ and $Perforin^{low/neg}$ NK subset that correlated with myeloid cell abundance in patients that are considered non-responders to anti-PD1 therapy from a published dataset (*30*). A recent study reported NK cells in lung tumors were associated with decreased MHC class II expression on DCs, which is consistent with our observations from NK cell/monocyte co-culture experiments. Furthermore, this study also reported cytokines being produced by NK cells within lung tumors and adjacent tissues and found that NK cells residing in normal lung tissues produce high amounts of IL-6 (*25*). Here, we confirm these results and demonstrate that breast cancer and sarcoma harbor IL-6 positive NK cells. We furthermore extend these observations demonstrating that the

Commented [DH91]: As per our style, we prefer the form 'patients with cancer' instead of 'cancer patients' in order to avoid identification of the subjects with the disease.

Commented [SYN92R91]: amended

Commented [DH93]: As per our style, we prefer the form 'patients with cancer' instead of 'cancer patients' in order to avoid identification of the subjects with the disease.

Commented [SYN94R93]: amended

frequency of IL-6 positive NK cells is associated with MHC class expression by tumor cells. However, the underlying trigger that initiates the production of IL-6 by NK cells remains unknown. Recent studies revealed that defective NK cell cytotoxicity is associated with the increased production of inflammatory cytokines (*61*-*63*). Still, the underlying cellular biology in which cytokine production is mechanistically influenced by NK cell killing capacity remains elusive.

In both patient cohorts and syngeneic mouse models, we found that IL-6 production by NK cells was elevated in tumors with high MHCI expression. Consistent with our *b2m*-KO tumor models, Bunting et al. demonstrated that MHCI expression in melanoma is associated with the deposition of extracellular proteins that dampens NK cell killing capacities and promote their production of inflammatory cytokines (*62*). NK cells within MHC class I-deficient RMA-S lymphoma tumors were also found to produce higher amounts of IFNγ (*63*). By either knocking out *B2M* in murine tumor cells or depleting the host NK cells, the frequencies of monocytic-MDSCs in the tumors were also reduced. In addition, we demonstrated that the prevalence of IL-6 deficient NK cells within the tumor microenvironment dampens tumor progression in contrast to tumors with WT NK cells. A recent study reported elevated production of human IL-6 upon tumor inoculation and immune checkpoint treatment of a humanized PDX model (*64*). Extending our investigations in similar xenograft models, targeting IL-6 by tocilizumab treatment or siRNA transfection in NK cells also reduced MDSC-mediated immune tolerance, further highlighting the role of IL-6 during NK cell to myeloid cell interactions within the TME.

Ultimately, the activation of MDSCs involve multiple inflammatory stimuli and growth factors (*65*). As such, it should be emphasized that IL-6 may not be the only driver for the

Commented [DH95]: Journal style avoids the use of the word “via”; please change to “through”, “by”, or similar.

Commented [SYN96R95]: amended

generation of MDSCs during the crosstalk with NK cells. From our transcriptomics analysis, tumor-experienced NK cells showed higher expression of *EBI3*, which encodes IL-35 and is known to cause accumulation of MDSCs and subsequent tumor angiogenesis (*66*). Moreover, higher frequencies of GM-CSF and TNFα-producing NK cells were observed in RMA tumors (*63*).

Our study has some limitations. Firstly, the influence of regulatory NK cells on myeloid cells could be spatially dependent which would require high dimensional spatial profiling approaches. Furthermore, such studies could incorporate a more comprehensive analysis to address the role of tumor MHC class I expression not only in relation to how NK cells influence myeloid cell populations, but also T cells. The second limitation would be the need for more sophisticated NK cell conditional knockout mice model to further substantiate our findings. Lastly, the immune profiling of sarcoma and breast tumors was performed with a limited phenotypic markers. By incorporating more NK cell markers in future immune profiling studies, we may better associate IL-6 production to any distinct maturation subset of NK cells.

To conclude, tumor resistance to cancer immune therapy can be ascribed to an inflamed yet poorly immunogenic microenvironment with the accumulation of tumor-associated NK cells and myeloid cells. Here, we provide multiple lines of evidence supporting the notion of tumor-associated NK cells indirectly suppressing cytotoxic T cells by causing the accumulation of myeloid suppressor cells within the TME. These findings highlight that the prevalence of NK cells in the tumor may not always be favorable. Consequently, NK cell functions should therefore be extensively characterized to dissect their roles in the microenvironment for each cancer type and between individual patients. Future efforts should

Commented [DH97]: Please include a limitations paragraph

Commented [SYN98R97]: we consolidated the limitations here into 3 main points. Hope this suffice.

consider modulating NK cells to prevent production of immune inhibitory factors, such as IL-6, or alternatively to produce factors that favor the development and recruitment of DCs. Understanding the functional plasticity of tumor-associated regulatory NK cells may inspire additional therapeutic avenues for the treatment of solid tumors.

Commented [DH99]: Author, correct?

Commented [SYN100R99]: ok

Materials and Methods

Study design

The present study was designed with the main objective of unravelling the capacity of regulatory NK cells to induce MDSCs. In particular, we focused on performing experiments that were specifically designed to demonstrate how tumor-experienced NK cells influence myeloid cell functions both in vitro and in vivo. Additionally, our study sought to be human-centred with the use of patient-derived xenografts, publicly available transcriptome datasets and flow cytometric analysis of freshly collected patient tissues. For murine and zebrafish studies, the co-investigators were blinded to the allocation of groups during data acquisition and subsequent analysis. Animals were randomized to minimize housing cage effects. Experimental and humane endpoints were determined by existing animal ethical permits approved for the present study.

Applicable to the use of both human and animal materials, data exclusion was determined based on the quality of samples collected, considering factors such as cell count and viability. In addition, failed experiments such as poor tumor engraftment in animals or low transfection efficiency of IL-6 knockdown in human primary NK cells were also excluded from downstream analysis. Despite that statistical methods were not used to predetermine sample size, sample sizes were decided based on prior experience on similar studies or pilot experiments. Sample sizes were ensured to achieve a greater than 95% probability of identifying effects by appropriate statistical analysis and at the same time, minimizing excessive usage of animals and human materials under ethical considerations. Sample sizes and choice of statistical tests are indicated in the figure legends and at the “Statistical analysis” section.

Study Approval

Commented [DH101]: Please make sure to include a study design paragraph with information on study size calculations, randomization, blinding, etc. If any of these were not performed, please indicate that as well. See manuscript revision checklist for details.

Commented [NSY102R101]: ok

Commented [DH103]: *Study design paragraph*. Include a separate section at the beginning of the Materials and Methods about the study design. It should contain:
Predefined study components (where applicable): Sample size justification (power analysis), rules for stopping data collection, data inclusion/exclusion criteria, treatment of outliers, endpoint selection method.
Rationale and design of study. Briefly (2–3 sentences) describe the overall objective and design of your study, including the treatments, the types of observations made, and the measurement techniques used.
Randomization. State whether the subjects or other experimental units were assigned randomly to the experimental groups and, if not, how the sample was selected.
Blinding. State whether the study was blinded, and the methods used for allocation concealment, blinded conduct of the experiment, and blinded assessment of outcomes.
Replication. Specify how many samples were used and how many experimental replicates were performed for each experiment. If this differs among experiments, include this information in the figure legend.
If your study falls into one of the categories listed in the EQUATOR Network library, follow the indicated reporting guidelines and note the appropriate guideline in your study design paragraph.

Commented [NSY104R103]: noted

Tumor resections were obtained from patients with breast cancer at Stockholm South General Hospital (Södersjukhuset) and Karolinska University Hospital. Tumor resections and peripheral blood were collected from patients with sarcoma at Karolinska University Hospital. Prior to resection, informed consent was given, and the collection of patient samples was approved by the ethical review board of Karolinska Institutet (2013/1979-31, 2016/957-31, 2017/742-32, and 2020-07099) and in accordance with the Declaration of Helsinki. Size of patient cohorts was dependent on the availability of tumor samples. Peripheral blood samples were obtained from purchased anonymized by-products of blood donations from healthy adult donors at the Karolinska University Hospital Blood Bank. Murine studies were conducted in accordance with approved animal ethical permits by the Swedish Board of Agriculture (11159-2018, 6197-2019) and by the Institutional Animal Care and Use Committee (IACUC, #221714) of A*STAR.

Commented [DH105]: As per our style, we prefer the form 'patients with cancer' instead of 'cancer patients' in order to avoid identification of the subjects with the disease.

Commented [SYN106R105]: amended

Processing of fresh tissue resections for tumor cell lines and TILs

Whole tumors were digested and processed with Tumor Dissociation Kit (Miltenyi Biotec). Tumor cells were then isolated by negative selection (Tumor Cell Isolation Kit, Miltenyi Biotec). Adherent cells were passaged at least five times before being used for experiments. All cell lines were maintained in RPMI1640 or in DMEM (Thermo Fisher Scientific) supplemented with 10% FBS (Thermo Fisher Scientific). To obtain TILs after tumor dissociation, cell suspensions were cultured in AIMV medium (Thermo Fisher Scientific) supplemented with 2.5% human AB serum and 3000 IU/ml of IL-15 (Peprotech). After 7 days, irradiated PBMCs were added at a ratio of 200:1 as feeder cells. Cultures were maintained with 500 IU/ml of IL-15 and functional grade antibody against CD3 (OKT3, Thermo Scientific). TILs were harvested after ten days for subsequent experiments.

Expansion cytokines were removed from cultures for at least 48 hours prior to any downstream experiments.

Tumor cell lines and chemicals

A summarized list of cell lines is provided as table S4. KADA and ANRU were previously established from primary melanoma tumor resections (*35*). BKT01 was established from breast cancer case 29 (Supplementary table 2). SK024 and SK051 were established from sarcoma cases 20 and 21 respectively (Supplementary table 3). All patient-derived cell lines were propagated and maintained in DMEM supplemented with 10% FBS whereas murine tumor cell lines Differentiated HepaRG (Biopredic) was maintained in hepaticult basal medium (Stem Cell technologies). SNU-475 (ATCC), HUH7 (JCRB), RMA, RMA-S and B16F10 (ATCC) were maintained in RPMI supplemented with 10% FBS. The generation of B16F10, 4T1 and MC38 cells with a knockout of *B2M* was established as previously described (*63*). List of purchased inhibitors with their respective experimental purposes are provided in table S5.

Isolation of peripheral blood mononuclear cells

Human peripheral blood mononuclear cells were collected through Ficoll density gradient centrifugation (GE Healthcare). Primary NK cells were isolated by negative selection following the manufacture protocol (Miltenyi Biotec, Human NK cells isolation kit), consistently yielding 95-99% purity based on flow cytometry analysis of CD3 negative and CD56 positive cells. Isolated NK cells were cultured in X-vivo 20 medium (Lonza) supplemented with 10% heat-inactivated human AB serum and 100 IU/mL of IL-2 (Proleukin) for 48 hours before subsequent co-culture experiments. Autologous monocytes were isolated by CD14-positive selection kit (Miltenyi Biotec). Based on reference protocol,

neutrophils were purified from fresh blood using the dextran sedimentation method after Ficoll density gradient centrifugation (*67*). In brief, 3% dextran (Sigma Aldrich) was added to red blood cell fraction after Ficoll separation to allow red blood cells to sediment within 30 minutes. Remaining white blood cells were subsequently washed with HBSS prior and analyzed for purity by flow cytometry.

In vitro generation of tumor-experienced NK cells

Isolated NK cells were cultured for 48-72 hours at 1:1 ratio with human tumor cell lines listed in supplementary table 4. After NK-tumor co-culture, tumor-experienced NK cells were sorted by flow cytometry based on CD45 expression for downstream experiments with either autologous neutrophils or monocytes. For controls, NK cells were either cultured alone in 10%FBS-RPMI media (control NK cells), tumor-supernatant or with non-tumor HepaRG cells.

Flow cytometry

Single-cell suspensions of PBMCs and tissue samples were washed with FACS buffer (5% FBS in PBS) before staining with antibody mixes (table S6 and S7) in the presence of Human Fc Block (BD Biosciences). For conventional flow cytometry, all samples were acquired on a Novocyte (ACEA Biosciences). Spectral flow cytometry was acquired on Cytek Aurora (Cytek Biosciences) (Phenotyping panel provided in table S8). All data were analyzed with FlowJo software (Tree Star). Intracellular staining of NK cell-derived IFNγ, IL-10, IL-4 and GM-CSF in patient samples was performed with respective cytokine catch/detection kits according to manufacturer's protocols (Miltenyi Biotec). After overnight incubation with the cytokine catch reagents, cells were treated overnight with Golgi-stop and Golgi-Plug (BD Biosciences) prior to the staining of surface markers and other intracellular

cytokines (IL-6 and TNFα). For the staining of phosphorylated proteins, cells were harvested after three days of NK cell-monocyte cultures or from dissociated xenograft tumor tissues. Staining was carried out with Cytofix/Phosflow buffer (BD Biosciences) according to manufacturer's protocols. Human NK cells were gated as negative for CD3 and positive for CD56. Annotated pie charts were generated by SPICE software developed by National Institutes of Health (NIH).

IL-6 RNA interference on primary isolated NK cells

Pre-designed siRNA constructs for IL-6 and control were obtained from Santa Cruz Biotechnology. Freshly isolated NK cells ($0.5x10^6$) were cultured overnight in serum-free AIMV media (Thermo Fisher Scientific) prior to transfection using Fuse-It-siRNA (IBIDI) according to the manufacturer's protocol. Three days later, the production of IL-6 was validated in NK cells stimulated with PMA/ionomycin. Since the transfection reagent can be detected by near-infrared fluorescence, transfected NK cells were FACS-sorted for downstream co-culture experiments with autologous monocytes. Of note, given the variable knockdown efficiency of IL-6 (fig. S6C) between donors, only NK cells from experiments with successful IL-6 knockdown were used in subsequent co-culture analysis.

Suppression Assay

$CD8^+$ T cells were isolated by negative selection based on the manufacturer's protocol (Human CD8 T Cell Isolation Kit, Miltenyi Biotec). Isolated $CD8^+$ T cells were labelled with 1 μM CFSE (BioLegend) and stimulated with 12 μl of CD3/CD28 beads (Thermo Fisher Scientific) per million cells and 50 IU/ml IL-2 for 48 hours before suppression assay. For the suppression assay, either monocytes or neutrophils were co-cultured with autologous

activated $CD8^+$ T cells at a suppressor to responder ratio of 1:10 in X-VIVO 20 media with 10% hAB serum. FACS analysis was performed after 48 hours of co-culture.

Antigen Presentation Assay

The evaluation of antigen presentation by allogenic, HLA-A2-phenotyped myeloid cells was adopted from a previous study using previously identified neo-epitopes derived from ANRU and KADA (*35*). In brief, control or tumor-experienced NK cells were first co-cultured with monocytes (1:10 ratio) for 48 hours prior to antigen priming with tumor lysate or 1µg/ml of neo-epitopes (MYLIP: KADA epitope; NUP210: ANRU). After 2 hours of priming with either KADA or ANRU-derived antigens, NK-monocytes cultures were washed and resuspended with either KADA or ANRU TILs (NK: Monocyte: TILs, 1:10:100) for an additional 48 hours. Subsequently, autologous tumor cells were added to the cultures (1:1 TIL: Tumor cell) for 4 hours of restimulation to test for IFNγ response by flow cytometry.

In vivo experiments

Male C57BL/6 mice at 7-week-old (Janvier labs and InVivos) were used for B16F10, MC38, RMA and RMA-S experiments. For B2m-KO B16F10 and MC38 tumor models, $0.1x10^6$ B16F10 cells or $1x10^6$ MC38 cells were resuspended in 50µl phosphate buffered saline (PBS) and injected subcutaneously into the right flank. For the B2m-KO 4T1 tumor model, $0.2x10^6$ 4T1 cells were injected into the mammary fat pad of 5-7 week-old female Balb/cAnNCrl mice (SCANBUR). For the RMA and RMA-S models, $0.1x10^6$ and $1x10^6$ cells were injected subcutaneously into the right flank respectively. Anti-NK1.1 neutralizing antibody (35mg/kg body weight, Custom produced by Mabtech) was intraperitoneally injected one day before tumor injection and then once per week (day 6 and 13). For experiment evaluating IL-6-KO NK cells, splenocytes were harvested from either WT or IL6-KO C57BL/6 mice (Jackson Laboratory) for murine NK cell isolation. From splenocytes,

murine NK cells were first isolated by negative selection-based commercial NK isolation kit (Miltenyi), followed by a second round of positive selection by using DX5 microbeads (Miltenyi). At day zero, $0.1x10^6$ B16F10 cells were subcutaneously co-injected together with $0.5\ x10^6$ WT or IL6-KO NK cells into the right flank of WT mice. In all tumor models, tumor growth was measured over time and the mice were sacrificed using a lethal dose of CO_2 after either experimental or humane endpoint was reached. Unless described otherwise in figure legend, experimental endpoints for B16F10 and RMA/RMA-S studies was 14 days post tumor inoculation while endpoints for MC38 and 4T1 were 18 days and 21 days post tumor inoculation respectively.

In-house bred NOD-scid-gamma (NSG) mice were 8-12 weeks old males. All mice were injected with $5x10^6$ melanoma cells (KADA cell line) subcutaneously into the right flank on day 0 suspended in 50% Matrigel (Corning) and 3000IU of IL-2. All mice then received an intravenous injection of $5x10^6$ TILs (autologous to tumor cells) together with $1x10^6$ monocytes on day 7. Groups 3 (G3) and 4 (G4) were injected with $1x10^6$ NK cells (autologous to monocytes) on day 0 together with tumor cells. Groups 2 (G2) and 4 (G4) were treated with 0.1 mg of Tocilizumab. Additional doses of tocilizumab (0,1mg) were given every 7 days intraperitoneally. Mice were sacrificed after 25 days for lung and primary tumor specimens for subsequent analysis (Figure 7D).

Commented [DH107]: What cell line?

Commented [SYN108R107]: amended

For tumor tissues, single cell suspensions were obtained for FACS analysis and human CD14 cell sorting using ARIA III fusion FACS sorter (BD). Sorted human CD14 cells were then used for subsequent suppression assay with autologous CD8 T cells as per described earlier.

Immunofluorescence

Fresh mouse lung tissues were embedded in OCT (VWR) and stored at -80°C. Lung tissues were cut into 10 µm thick sections. Slides were fixed in 4% paraformaldehyde (Merck) for 20 minutes and then blocked in 5% Bovine Serum Albumin (BSA, Sigma) in 0.1% Triton X100 (Sigma) PBS (Gibco) overnight at room temperature. HLA-ABC antibody (BD Pharmingen) and CD45 antibody (Abcam) were diluted to 1:200 in 1% BSA-PBS and added onto the slides at 4°C for overnight incubation. Alexa 555 donkey anti-rabbit IgG H+L antibody (Thermo Fisher Scientific), Alexa 647 donkey anti-mouse IgG H+L antibody (Thermo Fisher Scientific) and YO-PRO-1 (Thermo Fisher Scientific) were diluted to 1:400 in 1% BSA-DPBS. After rinsing in 0.1% Tween 20-DPBS for three times, sections were incubated with secondary antibodies and YO-PRO-1 at room temperature for 1 hour. Slides were then washed with 0.1% Tween 20-DPBS for three times. Slides were then mounted using fluoroshield with DAPI (Sigma) and covered by thin microscope coverslip for imaging under confocal microscopy. Up to three sections obtained from different z-stacks per lung specimen was analyzed under 5X objectives on Zeiss LSM800 confocal microscope. Using IMARIS software (Bitplane, Oxford Instruments), human tumor cells in the lungs were identified as HLA-ABC^{high} and CD45- cells with a minimum diameter of 15µm.

Commented [DH109]: Our style does not use trademarks, registered trademarks, copyright, etc. Please remove throughout

Commented [SYN110R109]: ok

Zebrafish Xenograft Tumor Model

KADA tumor cells were added in a pre-defined mixture (NK: Myeloid cells: TILs: Tumor cells; 1:10:100:100). TILs were pre-labelled (Red Dye) with Dil Stain whereastumor cells were labelled (Far-Red Dye) with DiD Cell labelling solution (Thermo Fisher Scientific). Experimental setup is illustrated in figure 6D. Zebrafish embryos at the age of 24 hpf (hours post fertilization) were incubated in water containing 0.2 mmol/L 1-phenyl-2-thio-urea (PTU, Sigma). At 48-hpf prior to microinjection, zebrafish embryos were dechorionated and anesthetized with 0.04 mg/mL of tricaine (MS-222, Sigma). The microinjection of human

cell mixture was performed by infusing 5nL (Approximately 500 cells in total) into the yolk sac of each larvaes using an Eppendorf microinjector (FemtoJet 5247, Eppendorf and Manipulator MM33-Right, Märzhäuser Wetziar). Successfully injected larvae were transferred into PTU aquarium water containing DAF-FM (5μM) at 33°C for 48 hours incubation before fixation with 4% paraformaldehyde (PFA) for image acquisition.

Fluorescent image acquisition and analysis

3D Images of zebrafish larvae were acquired by both Thunder Imaging System (Leica Microsystems) under 4X objectives and on Zeiss LSM800 confocal microscope under 10X objective. Batch quantification of different treatment groups were done using IMARIS software. (Bitplane, Oxford Instruments)

RNA sequencing of sorted NK cells

After co-culture with HepaRG or SNU475 cell lines for three days, purified NK cells were FACS-sorted by CD45 expression for subsequent bulk RNA sequencing. In brief, the sorted NK cells were frozen in in TRIzol (Thermo Fisher) and total RNA was extracted by acid guanidinium thiocyanate-phenol-chloroform extraction followed by a Qiagen RNeasy Micro clean-up procedure. RNA was quantified using RiboGreen (Thermo Fisher) and analyzed on Agilent Bioanalyser for quality assessment. cDNA libraries were prepared using 2 ng of total RNA using the Smart-seq2 protocol (*68*) with the following modifications: 1. Addition of 20 μM TSO; 2. Use of 200 pg cDNA with 1/5 reaction of Illumina Nextera XT kit. The length distribution of the cDNA libraries was monitored using a DNA High Sensitivity Reagent Kit on the Perkin Elmer Labchip. All samples were subjected to an indexed paired-end sequencing run of 2x151 cycles on an Illumina NovaSeq 6000 S4 flow cell, targeting 15 million reads per sample. Batch-corrected, normalised log2RPKM values (log2RPKM data

provided in table S9) were then processed for subsequent differential gene expression analysis on Partek Flow software (Partek) and geneset enrichment analysis performed on Cytoscape Cluego.

Transcriptomic analysis of public datasets

For the application of NK cell and inflammatory gene signatures, transcriptome data from immune checkpoint therapy patient datasets were downloaded from the NCBI Gene Expression Omnibus (GEO) database (GSE78220, GSE93157 and GSE165252). Three different NK gene signatures were obtained from previous studies (*27-29*). The inflammatory gene signature was originally derived from Buzzeo et. al. 2007 (*26*) For the inflammatory gene signature in supplementary table 1, genes upregulated as reported in the original study were selected and then filtered for immune-related genes based on the nCounter Pancancer 730-Immune Panel. Subsequently, a second round of manual filtering was done to select for genes involved in innate immunity. Genes related to T and NK cell activation were excluded from the inflammatory signature to avoid overlapping genes with any of the NK cell gene signatures for subsequent correlation analysis. Gene descriptions in supplementary table 1 were obtained from STRING consortium (accessed from: string-db.org). Gene signature scoring in each sample was quantified by a single-sample gene set enrichment analysis (ssGSEA) algorithm, performed by "GSVA" R package (*69*).

The anti-PD1 breast cancer single cell transcriptomics dataset was download from: http://biokey.lambrechtslab.org (*30*). With default setting on Partek Flow (Partek), raw count data was normalized prior to PCA, uMAP and tSNE dimensional reduction analysis. Myeloid cells were identified based on the original author's annotations before subclustering by the unsupervised louvain method for downstream differential gene expression analysis. NK cells

were manually annotated by the expression profile of KLRD1+, CD3E-, CD3D- and CD3G- within the original author's (T and NK) cluster. Similarly, the manually annotated NK cluster was then subdivided by the Louvain method into three subsets for gene expression analysis.

Statistical Analysis

Correlation matrixes were generated with custom R scripts and package "Corrplot". Kaplan-Meier analysis and log-rank test were conducted by R package "survminer" and "survival." All other experimental data were plotted and tested for significance using Prism 8.0 (GraphPad Software) as described in figure legends unless stated otherwise. *P* values below 0.05 were considered significant. Unless stated otherwise, all data presented are biological replicates with error bars representing the SD of the mean.

Supplementary materials

Figs. S1 to S10

Tables S1 to S9

MDAR Reproducibility Checklist

Data file S1

Commented [NSY111]: Updated accordingly

References

1. S. Kumagai, Y. Togashi, T. Kamada, E. Sugiyama, H. Nishinakamura, Y. Takeuchi, K. Vitaly, K. Itahashi, Y. Maeda, S. Matsui, T. Shibahara, Y. Yamashita, T. Irie, A. Tsuge, S. Fukuoka, A. Kawazoe, H. Udagawa, K. Kirita, K. Aokage, G. Ishii, T. Kuwata, K. Nakama, M. Kawazu, T. Ueno, N. Yamazaki, K. Goto, M. Tsuboi, H. Mano, T. Doi, K. Shitara, H. Nishikawa, The PD-1 expression balance between effector and regulatory T cells predicts the clinical efficacy of PD-1 blockade therapies. *Nat Immunol*, (2020); published online EpubAug 31 (10.1038/s41590-020-0769-3).
2. J. S. Lee, E. Ruppin, Multiomics Prediction of Response Rates to Therapies to Inhibit Programmed Cell Death 1 and Programmed Cell Death 1 Ligand 1. *JAMA Oncol*, (2019); published online EpubAug 22 (10.1001/jamaoncol.2019.2311).
3. J. E. Talmadge, D. I. Gabrilovich, History of myeloid-derived suppressor cells. *Nat Rev Cancer* **13**, 739-752 (2013); published online EpubOct (10.1038/nrc3581).
4. M. F. Al Sayed, M. A. Amrein, E. D. Buhrer, A. L. Huguenin, R. Radpour, C. Riether, A. F. Ochsenbein, T-cell-Secreted TNFalpha Induces Emergency Myelopoiesis and Myeloid-Derived Suppressor Cell Differentiation in Cancer. *Cancer Res* **79**, 346-359 (2019); published online EpubJan 15 (10.1158/0008-5472.CAN-17-3026).
5. S. L. Highfill, Y. Cui, A. J. Giles, J. P. Smith, H. Zhang, E. Morse, R. N. Kaplan, C. L. Mackall, Disruption of CXCR2-mediated MDSC tumor trafficking enhances anti-PD1 efficacy. *Sci Transl Med* **6**, 237ra267 (2014); published online EpubMay 21 (10.1126/scitranslmed.3007974).
6. T. Baumann, A. Dunkel, C. Schmid, S. Schmitt, M. Hiltensperger, K. Lohr, V. Laketa, S. Donakonda, U. Ahting, B. Lorenz-Depiereux, J. E. Heil, J. Schredelseker, L. Simeoni, C. Fecher, N. Korber, T. Bauer, N. Huser, D. Hartmann, M. Laschinger, K. Eyerich, S. Eyerich, M. Anton, M. Streeter, T. Wang, B. Schraven, D. Spiegel, F. Assaad, T. Misgeld, H. Zischka, P. J. Murray, A. Heine, M. Heikenwalder, T. Korn, C. Dawid, T. Hofmann, P. A. Knolle, B. Hochst, Regulatory myeloid cells paralyze T cells through cell-cell transfer of the metabolite methylglyoxal. *Nat Immunol* **21**, 555-566 (2020); published online EpubMay (10.1038/s41590-020-0666-9).
7. S. Nagaraj, A. G. Schrum, H. I. Cho, E. Celis, D. I. Gabrilovich, Mechanism of T cell tolerance induced by myeloid-derived suppressor cells. *J Immunol* **184**, 3106-3116 (2010); published online EpubMar 15 (10.4049/jimmunol.0902661).
8. I. Poschke, D. Mougiakakos, J. Hansson, G. V. Masucci, R. Kiessling, Immature immunosuppressive CD14+HLA-DR-/low cells in melanoma patients are Stat3hi and overexpress CD80, CD83, and DC-sign. *Cancer Res* **70**, 4335-4345 (2010); published online EpubJun 1 (10.1158/0008-5472.CAN-09-3767).
9. B. Dawod, J. Liu, S. Gebremeskel, C. Yan, A. Sappong, B. Johnston, D. W. Hoskin, J. S. Marshall, J. Wang, Myeloid-derived suppressor cell depletion therapy targets IL-17A-expressing mammary carcinomas. *Sci Rep* **10**, 13343 (2020); published online EpubAug 7 (10.1038/s41598-020-70231-7).
10. S. Hegde, A. M. Leader, M. Merad, MDSC: Markers, development, states, and unaddressed complexity. *Immunity* **54**, 875-884 (2021); published online EpubMay 11 (10.1016/j.immuni.2021.04.004).
11. E. Vivier, S. Ugolini, Regulatory natural killer cells: new players in the IL-10 anti-inflammatory response. *Cell Host Microbe* **6**, 493-495 (2009); published online EpubDec 17 (10.1016/j.chom.2009.12.001).

Commented [DH112]: References must be in the correct style: All authors should be cited, title of article, Journal Name 15 [vol], 444-450 [page range] (2010) [year of publication]. STM follows the same style as Science Signaling in EndNote.

Commented [SYN113R112]: We have updated to the science signaling style using endnote.

12. C. Louis, F. Souza-Fonseca-Guimaraes, Y. Yang, D. D'Silva, T. Kratina, L. Dagley, S. Hediyeh-Zadeh, J. Rautela, S. L. Masters, M. J. Davis, J. J. Babon, B. Ciric, E. Vivier, W. S. Alexander, N. D. Huntington, I. P. Wicks, NK cell-derived GM-CSF potentiates inflammatory arthritis and is negatively regulated by CIS. *J Exp Med* **217**, (2020); published online EpubMay 4 (10.1084/jem.20191421).
13. S. Y. Neo, Y. Yang, J. Record, R. Ma, X. Chen, Z. Chen, N. P. Tobin, E. Blake, C. Seitz, R. Thomas, A. K. Wagner, J. Andersson, J. de Boniface, J. Bergh, S. Murray, E. Alici, R. Childs, M. Johansson, L. S. Westerberg, F. Haglund, J. Hartman, A. Lundqvist, CD73 immune checkpoint defines regulatory NK cells within the tumor microenvironment. *J Clin Invest* **130**, 1185-1198 (2020); published online EpubMar 2 (10.1172/JCI128895).
14. C. Fauriat, E. O. Long, H. G. Ljunggren, Y. T. Bryceson, Regulation of human NK-cell cytokine and chemokine production by target cell recognition. *Blood* **115**, 2167-2176 (2010); published online EpubMar 18 (10.1182/blood-2009-08-238469).
15. L. Dolcetti, E. Peranzoni, S. Ugel, I. Marigo, A. Fernandez Gomez, C. Mesa, M. Geilich, G. Winkels, E. Traggiai, A. Casati, F. Grassi, V. Bronte, Hierarchy of immunosuppressive strength among myeloid-derived suppressor cell subsets is determined by GM-CSF. *Eur J Immunol* **40**, 22-35 (2010); published online EpubJan (10.1002/eji.200939903).
16. K. Maeda, A. Malykhin, B. N. Teague-Weber, X. H. Sun, A. D. Farris, K. M. Coggeshall, Interleukin-6 aborts lymphopoiesis and elevates production of myeloid cells in systemic lupus erythematosus-prone B6.Sle1.Yaa animals. *Blood* **113**, 4534-4540 (2009); published online EpubMay 7 (10.1182/blood-2008-12-192559).
17. I. Bah, A. Kumbhare, L. Nguyen, C. E. McCall, M. El Gazzar, IL-10 induces an immune repressor pathway in sepsis by promoting S100A9 nuclear localization and MDSC development. *Cell Immunol* **332**, 32-38 (2018); published online EpubOct (10.1016/j.cellimm.2018.07.003).
18. K. M. Hart, K. T. Byrne, M. J. Molloy, E. M. Usherwood, B. Berwin, IL-10 immunomodulation of myeloid cells regulates a murine model of ovarian cancer. *Front Immunol* **2**, 29 (2011)10.3389/fimmu.2011.00029).
19. M. A. Clavijo-Salomon, R. Salcedo, S. Roy, R. X. das Neves, A. Dzutsev, H. Sales-Campos, K. S. Borbely, L. Silla, J. S. Orange, E. M. Mace, J. A. M. Barbuto, G. Trinchieri, Human NK cells prime inflammatory DC precursors to induce Tc17 differentiation. *Blood Adv* **4**, 3990-4006 (2020); published online EpubAug 25 (10.1182/bloodadvances.2020002084).
20. M. A. Cooper, T. A. Fehniger, A. Fuchs, M. Colonna, M. A. Caligiuri, NK cell and DC interactions. *Trends Immunol* **25**, 47-52 (2004); published online EpubJan (10.1016/j.it.2003.10.012).
21. A. Bruno, L. Mortara, D. Baci, D. M. Noonan, A. Albini, Myeloid Derived Suppressor Cells Interactions With Natural Killer Cells and Pro-angiogenic Activities: Roles in Tumor Progression. *Front Immunol* **10**, 771 (2019)10.3389/fimmu.2019.00771).
22. C. Munz, T. Dao, G. Ferlazzo, M. A. de Cos, K. Goodman, J. W. Young, Mature myeloid dendritic cell subsets have distinct roles for activation and viability of circulating human natural killer cells. *Blood* **105**, 266-273 (2005); published online EpubJan 1 (10.1182/blood-2004-06-2492).
23. S. Welte, S. Kuttruff, I. Waldhauer, A. Steinle, Mutual activation of natural killer cells and monocytes mediated by NKp80-AICL interaction. *Nat Immunol* **7**, 1334-1342 (2006); published online EpubDec (10.1038/ni1402).

24. N. Dalbeth, R. Gundle, R. J. Davies, Y. C. Lee, A. J. McMichael, M. F. Callan, CD56bright NK cells are enriched at inflammatory sites and can engage with monocytes in a reciprocal program of activation. *J Immunol* **173**, 6418-6426 (2004); published online EpubNov 15 (10.4049/jimmunol.173.10.6418).
25. J. Russick, P. E. Joubert, M. Gillard-Bocquet, C. Torset, M. Meylan, F. Petitprez, M. A. Dragon-Durey, S. Marmier, A. Varthaman, N. Josseaume, C. Germain, J. Goc, M. C. Dieu-Nosjean, P. Validire, L. Fournel, L. Zitvogel, G. Bindea, A. Lupo, D. Damotte, M. Alifano, I. Cremer, Natural killer cells in the human lung tumor microenvironment display immune inhibitory functions. *J Immunother Cancer* **8**, (2020); published online EpubOct (10.1136/jitc-2020-001054).
26. M. P. Buzzeo, J. Yang, G. Casella, V. Reddy, Hematopoietic stem cell mobilization with G-CSF induces innate inflammation yet suppresses adaptive immune gene expression as revealed by microarray analysis. *Exp Hematol* **35**, 1456-1465 (2007); published online EpubSep (10.1016/j.exphem.2007.06.001).
27. J. P. Bottcher, E. Bonavita, P. Chakravarty, H. Blees, M. Cabeza-Cabrerizo, S. Sammicheli, N. C. Rogers, E. Sahai, S. Zelenay, E. S. C. Reis, NK Cells Stimulate Recruitment of cDC1 into the Tumor Microenvironment Promoting Cancer Immune Control. *Cell* **172**, 1022-1037 e1014 (2018); published online EpubFeb 22 (10.1016/j.cell.2018.01.004).
28. X. Zheng, Y. Qian, B. Fu, D. Jiao, Y. Jiang, P. Chen, Y. Shen, H. Zhang, R. Sun, Z. Tian, H. Wei, Mitochondrial fragmentation limits NK cell-based tumor immunosurveillance. *Nat Immunol* **20**, 1656-1667 (2019); published online EpubDec (10.1038/s41590-019-0511-1).
29. J. Cursons, F. Souza-Fonseca-Guimaraes, M. Foroutan, A. Anderson, F. Hollande, S. Hediyeh-Zadeh, A. Behren, N. D. Huntington, M. J. Davis, A Gene Signature Predicting Natural Killer Cell Infiltration and Improved Survival in Melanoma Patients. *Cancer Immunol Res* **7**, 1162-1174 (2019); published online EpubJul (10.1158/2326-6066.CIR-18-0500).
30. A. Bassez, H. Vos, L. Van Dyck, G. Floris, I. Arijs, C. Desmedt, B. Boeckx, M. Vanden Bempt, I. Nevelsteen, K. Lambein, K. Punie, P. Neven, A. D. Garg, H. Wildiers, J. Qian, A. Smeets, D. Lambrechts, A single-cell map of intratumoral changes during anti-PD1 treatment of patients with breast cancer. *Nat Med* **27**, 820-832 (2021); published online EpubMay (10.1038/s41591-021-01323-8).
31. H. Li, N. Zhai, Z. Wang, H. Song, Y. Yang, A. Cui, T. Li, G. Wang, J. Niu, I. N. Crispe, L. Su, Z. Tu, Regulatory NK cells mediated between immunosuppressive monocytes and dysfunctional T cells in chronic HBV infection. *Gut* **67**, 2035-2044 (2018); published online EpubNov (10.1136/gutjnl-2017-314098).
32. Y. Pico de Coana, M. Wolodarski, I. van der Haar Avila, T. Nakajima, S. Rentouli, A. Lundqvist, G. Masucci, J. Hansson, R. Kiessling, PD-1 checkpoint blockade in advanced melanoma patients: NK cells, monocytic subsets and host PD-L1 expression as predictive biomarker candidates. *Oncoimmunology* **9**, 1786888 (2020); published online EpubAug 28 (10.1080/2162402X.2020.1786888).
33. V. Bronte, S. Brandau, S. H. Chen, M. P. Colombo, A. B. Frey, T. F. Greten, S. Mandruzzato, P. J. Murray, A. Ochoa, S. Ostrand-Rosenberg, P. C. Rodriguez, A. Sica, V. Umansky, R. H. Vonderheide, D. I. Gabrilovich, Recommendations for myeloid-derived suppressor cell nomenclature and characterization standards. *Nat Commun* **7**, 12150 (2016); published online EpubJul 6 (10.1038/ncomms12150).
34. D. I. Gabrilovich, J. Corak, I. F. Ciernik, D. Kavanaugh, D. P. Carbone, Decreased antigen presentation by dendritic cells in patients with breast cancer. *Clin Cancer Res* **3**, 483-490 (1997); published online EpubMar (

35. S. L. Wickstrom, T. Lovgren, M. Volkmar, B. Reinhold, J. S. Duke-Cohan, L. Hartmann, J. Rebmann, A. Mueller, J. Melief, R. Maas, M. Ligtenberg, J. Hansson, R. Offringa, B. Seliger, I. Poschke, E. L. Reinherz, R. Kiessling, Cancer Neoepitopes for Immunotherapy: Discordance Between Tumor-Infiltrating T Cell Reactivity and Tumor MHC Peptidome Display. *Frontiers in Immunology* **10**, (2019); published online EpubDec 11 (ARTN 2766 10.3389/fimmu.2019.02766).
36. P. T. Thevenot, R. A. Sierra, P. L. Raber, A. A. Al-Khami, J. Trillo-Tinoco, P. Zarreii, A. C. Ochoa, Y. Cui, L. Del Valle, P. C. Rodriguez, The stress-response sensor chop regulates the function and accumulation of myeloid-derived suppressor cells in tumors. *Immunity* **41**, 389-401 (2014); published online EpubSep 18 (10.1016/j.immuni.2014.08.015).
37. T. Condamine, V. Kumar, I. R. Ramachandran, J. I. Youn, E. Celis, N. Finnberg, W. S. El-Deiry, R. Winograd, R. H. Vonderheide, N. R. English, S. C. Knight, H. Yagita, J. C. McCaffrey, S. Antonia, N. Hockstein, R. Witt, G. Masters, T. Bauer, D. I. Gabrilovich, ER stress regulates myeloid-derived suppressor cell fate through TRAIL-R-mediated apoptosis. *J Clin Invest* **124**, 2626-2639 (2014); published online EpubJun (10.1172/JCI74056).
38. S. Goswami, T. Walle, A. E. Cornish, S. Basu, S. Anandhan, I. Fernandez, L. Vence, J. Blando, H. Zhao, S. S. Yadav, M. Ott, L. Y. Kong, A. B. Heimberger, J. de Groot, B. Sepesi, M. Overman, S. Kopetz, J. P. Allison, D. Pe'er, P. Sharma, Immune profiling of human tumors identifies CD73 as a combinatorial target in glioblastoma. *Nat Med* **26**, 39-46 (2020); published online EpubJan (10.1038/s41591-019-0694-x).
39. M. D. Bern, B. A. Parikh, L. Yang, D. L. Beckman, J. Poursine-Laurent, W. M. Yokoyama, Inducible down-regulation of MHC class I results in natural killer cell tolerance. *J Exp Med* **216**, 99-116 (2019); published online EpubJan 7 (10.1084/jem.20181076).
40. J. Renn, B. Pruvot, M. Muller, Detection of nitric oxide by diaminofluorescein visualizes the skeleton in living zebrafish. *J Appl Ichthyol* **30**, 701-706 (2014); published online EpubAug (10.1111/jai.12514).
41. Y. P. de Coana, M. Wolodarski, I. Poschke, Y. Yoshimoto, Y. Yang, M. Nystrom, U. Edback, S. E. Brage, A. Lundqvist, G. V. Masucci, J. Hansson, R. Kiessling, Ipilimumab treatment decreases monocytic MDSCs and increases CD8 effector memory T cells in long-term survivors with advanced melanoma. *Oncotarget* **8**, 21539-21553 (2017); published online EpubMar 28 (10.18632/oncotarget.15368).
42. C. Meyer, L. Cagnon, C. M. Costa-Nunes, P. Baumgaertner, N. Montandon, L. Leyvraz, O. Michielin, E. Romano, D. E. Speiser, Frequencies of circulating MDSC correlate with clinical outcome of melanoma patients treated with ipilimumab. *Cancer Immunol Immunother* **63**, 247-257 (2014); published online EpubMar (10.1007/s00262-013-1508-5).
43. O. De Henau, M. Rausch, D. Winkler, L. F. Campesato, C. Liu, D. H. Cymerman, S. Budhu, A. Ghosh, M. Pink, J. Tchaicha, M. Douglas, T. Tibbitts, S. Sharma, J. Proctor, N. Kosmider, K. White, H. Stern, J. Soglia, J. Adams, V. J. Palombella, K. McGovern, J. L. Kutok, J. D. Wolchok, T. Merghoub, Overcoming resistance to checkpoint blockade therapy by targeting PI3Kgamma in myeloid cells. *Nature* **539**, 443-447 (2016); published online EpubNov 17 (10.1038/nature20554).
44. K. Kim, A. D. Skora, Z. Li, Q. Liu, A. J. Tam, R. L. Blosser, L. A. Diaz, Jr., N. Papadopoulos, K. W. Kinzler, B. Vogelstein, S. Zhou, Eradication of metastatic mouse cancers resistant to immune checkpoint blockade by suppression of myeloid-

derived cells. *Proc Natl Acad Sci U S A* **111**, 11774-11779 (2014); published online EpubAug 12 (10.1073/pnas.1410626111).
45. L. Tong, C. Jimenez-Cortegana, A. H. M. Tay, S. Wickstrom, L. Galluzzi, A. Lundqvist, NK cells and solid tumors: therapeutic potential and persisting obstacles. *Molecular cancer* **21**, 206 (2022); published online EpubNov 1 (10.1186/s12943-022-01672-z).
46. D. Bruni, H. K. Angell, J. Galon, The immune contexture and Immunoscore in cancer prognosis and therapeutic efficacy. *Nat Rev Cancer* **20**, 662-680 (2020); published online EpubNov (10.1038/s41568-020-0285-7).
47. S. Nersesian, S. L. Schwartz, S. R. Grantham, L. K. MacLean, S. N. Lee, M. Pugh-Toole, J. E. Boudreau, NK cell infiltration is associated with improved overall survival in solid cancers: A systematic review and meta-analysis. *Transl Oncol* **14**, 100930 (2021); published online EpubJan (10.1016/j.tranon.2020.100930).
48. F. Veglia, E. Sanseviero, D. I. Gabrilovich, Myeloid-derived suppressor cells in the era of increasing myeloid cell diversity. *Nat Rev Immunol*, (2021); published online EpubFeb 1 (10.1038/s41577-020-00490-y).
49. C. Menetrier-Caux, M. C. Thomachot, L. Alberti, G. Montmain, J. Y. Blay, IL-4 prevents the blockade of dendritic cell differentiation induced by tumor cells. *Cancer Res* **61**, 3096-3104 (2001); published online EpubApr 1 (
50. Z. Zhou, D. L. French, G. Ma, S. Eisenstein, Y. Chen, C. M. Divino, G. Keller, S. H. Chen, P. Y. Pan, Development and function of myeloid-derived suppressor cells generated from mouse embryonic and hematopoietic stem cells. *Stem Cells* **28**, 620-632 (2010); published online EpubMar 31 (10.1002/stem.301).
51. I. Marigo, E. Bosio, S. Solito, C. Mesa, A. Fernandez, L. Dolcetti, S. Ugel, N. Sonda, S. Bicciato, E. Falisi, F. Calabrese, G. Basso, P. Zanovello, E. Cozzi, S. Mandruzzato, V. Bronte, Tumor-induced tolerance and immune suppression depend on the C/EBPbeta transcription factor. *Immunity* **32**, 790-802 (2010); published online EpubJun 25 (10.1016/j.immuni.2010.05.010).
52. M. G. Lechner, D. J. Liebertz, A. L. Epstein, Characterization of cytokine-induced myeloid-derived suppressor cells from normal human peripheral blood mononuclear cells. *J Immunol* **185**, 2273-2284 (2010); published online EpubAug 15 (10.4049/jimmunol.1000901).
53. Y. Mao, D. Sarhan, A. Steven, B. Seliger, R. Kiessling, A. Lundqvist, Inhibition of tumor-derived prostaglandin-e2 blocks the induction of myeloid-derived suppressor cells and recovers natural killer cell activity. *Clin Cancer Res* **20**, 4096-4106 (2014); published online EpubAug 1 (10.1158/1078-0432.CCR-14-0635).
54. K. C. Barry, J. Hsu, M. L. Broz, F. J. Cueto, M. Binnewies, A. J. Combes, A. E. Nelson, K. Loo, R. Kumar, M. D. Rosenblum, M. D. Alvarado, D. M. Wolf, D. Bogunovic, N. Bhardwaj, A. I. Daud, P. K. Ha, W. R. Ryan, J. L. Pollack, B. Samad, S. Asthana, V. Chan, M. F. Krummel, A natural killer-dendritic cell axis defines checkpoint therapy-responsive tumor microenvironments. *Nat Med* **24**, 1178-1191 (2018); published online EpubAug (10.1038/s41591-018-0085-8).
55. O. Melaiu, M. Chierici, V. Lucarini, G. Jurman, L. A. Conti, R. De Vito, R. Boldrini, L. Cifaldi, A. Castellano, C. Furlanello, V. Barnaba, F. Locatelli, D. Fruci, Cellular and gene signatures of tumor-infiltrating dendritic cells and natural-killer cells predict prognosis of neuroblastoma. *Nat Commun* **11**, 5992 (2020); published online EpubNov 25 (10.1038/s41467-020-19781-y).
56. S. Q. Crome, L. T. Nguyen, S. Lopez-Verges, S. Y. Yang, B. Martin, J. Y. Yam, D. J. Johnson, J. Nie, M. Pniak, P. H. Yen, A. Milea, R. Sowamber, S. R. Katz, M. Q. Bernardini, B. A. Clarke, P. A. Shaw, P. A. Lang, H. K. Berman, T. J. Pugh, L. L.

Lanier, P. S. Ohashi, A distinct innate lymphoid cell population regulates tumor-associated T cells. *Nat Med* **23**, 368-375 (2017); published online EpubMar (10.1038/nm.4278).

57. G. Perona-Wright, K. Mohrs, F. M. Szaba, L. W. Kummer, R. Madan, C. L. Karp, L. L. Johnson, S. T. Smiley, M. Mohrs, Systemic but not local infections elicit immunosuppressive IL-10 production by natural killer cells. *Cell Host Microbe* **6**, 503-512 (2009); published online EpubDec 17 (10.1016/j.chom.2009.11.003).
58. I. S. Chan, H. Knutsdottir, G. Ramakrishnan, V. Padmanaban, M. Warrier, J. C. Ramirez, M. Dunworth, H. Zhang, E. M. Jaffee, J. S. Bader, A. J. Ewald, Cancer cells educate natural killer cells to a metastasis-promoting cell state. *J Cell Biol* **219**, (2020); published online EpubSep 7 (10.1083/jcb.202001134).
59. S. Rezaeifard, A. Talei, M. Shariat, N. Erfani, Tumor infiltrating NK cell (TINK) subsets and functional molecules in patients with breast cancer. *Mol Immunol* **136**, 161-167 (2021); published online EpubAug (10.1016/j.molimm.2021.03.003).
60. P. Li, M. Lu, J. Shi, L. Hua, Z. Gong, Q. Li, L. D. Shultz, G. Ren, Dual roles of neutrophils in metastatic colonization are governed by the host NK cell status. *Nat Commun* **11**, 4387 (2020); published online EpubSep 1 (10.1038/s41467-020-18125-0).
61. M. Anft, P. Netter, D. Urlaub, I. Prager, S. Schaffner, C. Watzl, NK cell detachment from target cells is regulated by successful cytotoxicity and influences cytokine production. *Cell Mol Immunol* **17**, 347-355 (2020); published online EpubApr (10.1038/s41423-019-0277-2).
62. M. D. Bunting, M. Vyas, M. Requesens, A. Langenbucher, E. B. Schiferle, R. T. Manguso, M. S. Lawrence, S. Demehri, Extracellular matrix proteins regulate NK cell function in peripheral tissues. *Sci Adv* **8**, eabk3327 (2022); published online EpubMar 18 (10.1126/sciadv.abk3327).
63. S. Y. Neo, X. Jing, L. Tong, D. Tong, J. Gao, Z. Chen, M. C. De Los Santos, N. Burduli, S. De Souza Ferreira, A. K. Wagner, E. Alici, C. Rolny, Y. Cao, A. Lundqvist, Tumor MHC class I expression alters cancer-associated myelopoiesis driven by host NK cells. *J Immunother Cancer* **10**, (2022); published online EpubOct (10.1136/jitc-2022-005308).
64. W. N. Liu, S. Y. Fong, W. W. S. Tan, S. Y. Tan, M. Liu, J. Y. Cheng, S. Lim, L. Suteja, E. K. Huang, J. K. Y. Chan, N. G. Iyer, J. P. S. Yeong, D. W. Lim, Q. Chen, Establishment and Characterization of Humanized Mouse NPC-PDX Model for Testing Immunotherapy. *Cancers (Basel)* **12**, (2020); published online EpubApr 22 (10.3390/cancers12041025).
65. T. Condamine, D. I. Gabrilovich, Molecular mechanisms regulating myeloid-derived suppressor cell differentiation and function. *Trends Immunol* **32**, 19-25 (2011); published online EpubJan (10.1016/j.it.2010.10.002).
66. Z. Wang, J. Q. Liu, Z. Liu, R. Shen, G. Zhang, J. Xu, S. Basu, Y. Feng, X. F. Bai, Tumor-derived IL-35 promotes tumor growth by enhancing myeloid cell accumulation and angiogenesis. *J Immunol* **190**, 2415-2423 (2013); published online EpubMar 1 (10.4049/jimmunol.1202535).
67. D. B. Kuhns, D. A. L. Priel, J. Chu, K. A. Zarember, Isolation and Functional Analysis of Human Neutrophils. *Curr Protoc Immunol* **111**, 7 23 21-27 23 16 (2015); published online EpubNov 2 (10.1002/0471142735.im0723s111).
68. S. Picelli, O. R. Faridani, A. K. Bjorklund, G. Winberg, S. Sagasser, R. Sandberg, Full-length RNA-seq from single cells using Smart-seq2. *Nat Protoc* **9**, 171-181 (2014); published online EpubJan (10.1038/nprot.2014.006).

69. S. Hanzelmann, R. Castelo, J. Guinney, GSVA: gene set variation analysis for microarray and RNA-seq data. *BMC Bioinformatics* **14**, 7 (2013); published online EpubJan 16 (10.1186/1471-2105-14-7).

Acknowledgements

We thank A. Malmerfelt, J. Teo, B. Aw, A. Kurzay and D. Sarhan for technical assistance and intellectual input. We thank J. Zhao and H. Yu for the courtesy of HepaRG cells. We also thank the Immunogenomics, Computational Immunology Core (SIgN, ASTAR), animal facilities (BRC, ASTAR and KM-B and -F, Karolinska Institutet), Bioimaging core (BIC, Karolinska Institutet), Zebrafish core (Karolinska Institutet), and flow cytometry core facilities (BFC, Karolinska Institutet and SIgN, ASTAR). All illustrations were created with BioRender.com.

Funding

This work is supported by A*STAR SIgN core funds, The National Research Foundation of Singapore (NRF-CRP26-2021RS-0001 to SX and KPL, NRF2017_SISFP09 to KPL), The Swedish Cancer Society (#21 1524 Pj to AL, #190104Pj01H and #190108Us01H to RK), The Cancer Research Foundations of Radiumhemmet (#211253 to AL and #194123 to RK), The Swedish Research Council (#2019-01212 to RK and #2022-00723 to AL), The Swedish Childhood Cancer Foundation (PR2021-0039 to AL), and the Stockholm City Council (LS 2018-1157 to RK).

Commented [DH114]: Grants numbers should be listed along with the appropriate author's initials. State initials of recipient after each grant number (e.g. `to YX').

Commented [NSY115R114]: Ok

Author Contributions

S.Y.N and A.L conceptualized and led the study. S.Y.N, L.T, J.C and Z.C performed in vitro experiments on human NK cells and downstream flow cytometric analysis. N.B and A.K.W generated B2M-KO cell lines for murine studies. S.Y.N, L.T, J.C, Y.L, X.J, M.M.O, K.L, J.G and J.H are involved with in vivo mice experiments and subsequent data acquisition. L.T, Z.C and J.P.L performed the in vivo zebrafish experiments and confocal imaging. S.Y.N and Y.C performed transcriptomics analyses on in-house generated and public-available datasets. S.Y.N, L.T and S.L.W generated patient-derived tumor cell lines. S.L.W, X.C, R.M, F.H and J.H acquired patient samples for downstream processing and data acquisition. S.X, E.A, Y.C,

Commented [DH116]: Please make sure that all authors' contributions are accounted for. Please make sure that all authors' contributions are accounted for. A complete list of contributions by each author to the paper (such as: X.X. designed the experiments. X.X. provided funding and wrote the paper). This should be in complete sentences in a paragraph. This should be as detailed as possible so as to include which authors performed which experiments (in vivo, in vitro, flow, etc.)

Commented [NSY117R116]: Ok noted

R.K, K.P.L, L.S.W and A.L contributed to funding acquisition and project administration. S.Y.N and A.L performed data interpretation and wrote the manuscript. All authors contributed research inputs, reviewed and approved the manuscript.

Competing Interests

JH is a co-founder and shareholder of Stratipath AB. JH has obtained institutional research support from Novartis and Cepheid. JH has been at advisory boards at Roche, Novartis, MSD, Merck and Eli Lilly. Speakers' bureau at Pfizer, Novartis. Abovementioned are declared not related to the present work.

Data and materials availability

All data associated with this study are present in the paper or supplementary materials. CRISPR vectors, non-commercial and modified cell lines are available upon reasonable request through material transfer agreements with Karolinska Institute, Sweden.

Commented [DH118]: All consulting, whether paid or unpaid, and whether related to the present work or not, needs to be declared here. Any patents related to this work need to be stated here (cite patent title and filing #).

Commented [SYN119R118]: amended

Commented [DH120]: Please verify no other data must be publicly uploaded: The following types of data must be submitted to an appropriate database before acceptance:-DNA sequence data -Atomic coordinates and structure factor files or electron microscopy maps for molecular structures -Microarray data in MIAME compliant form -Small-molecule crystallographic data -Protein and molecular interaction data -Computer code See for details and approved databases. Please state whether any proprietary materials that are not otherwise available would need to be provided to readers using an MTA. Please explicitly state which materials would be provided by the authors under a material transfer agreement and please provide a blank MTA for our records.

Commented [NSY121R120]: ok

Figure Legends

Figure 1. A unique inflammatory gene signature correlate with NK cell signature in non-responders to immune checkpoint blockade

(A) Hierarchical clustering heatmap showing genes within the inflammatory signature with increasing NK score in a batch corrected pool of three cohorts of 128 patients (See Fig S1A for details) receiving immune checkpoint therapy. (B) Correlation of NK and inflammatory gene signature scores grouped based on pre-defined responders and non-responders to therapy in the esophageal tumor cohort (GSE165252) on baseline samples (n=32). **(C)** Correlation of NK and inflammatory gene signature scores grouped based on pre-defined responders and non-responders to therapy in the esophageal tumor cohort (GSE165252) for on-treatment samples (n=29). **(D)** Correlation of NK and inflammatory gene signature score grouped based on pre-defined responders and non-responders to therapy in a pembrolizumab melanoma cohort (GSE78220, n=28). **(E)** Correlation of NK and inflammatory gene signature score grouped based on the RECIST response criteria in the mixed tumor cohort (GSE93157, n=65). PD: Progressive Disease, CR: Complete Response, PR: Partial Response and SD: Stable Disease.**(B to E)** NK gene signature (*Bottcher* et al. 2018) was used for correlation analysis. Pearson correlation was performed for all correlation analysis. ns=non-significant, **P*<0.05, ***P*<0.01 and *****P*<0.0001. **(F)** UMAP projections of myeloid subsets defined in tumors from a public dataset of patients with breast cancer and receiving anti-PD1 therapy in which patients (n=29) were grouped based on the presence of clonal expansion of T cells in response to therapy. Unsupervised clustering of myeloid cells was performed with the Louvain method. **(G)** UMAP projections of myeloid subsets with normalized expression of 6 distinct myeloid genes defining various macrophages and monocyte subsets. **(H)** Spearman Correlation matrix showing the

Commented [DH122]: Figure legends should be a single paragraph

Commented [NSY123R122]: ok

Commented [DH124]: What cohort is this?

Commented [NSY125R124]: Amended with more details

Commented [DH126]: All subfigures need to introduced seperately

Commented [NSY127R126]: noted

relationship between the abundance of various myeloid and NK cell subsets in patient tumors with or without T cell clonal expansion in response to anti-PD1 therapy.

Figure 2. **Tumor-experienced NK cells acquire a CD69+, perforin- phenotype with transcriptional reprogramming for immune-regulatory function.**

(A) uMAP projection of various defined NK cell subsets and expression of CD69 and perforin based on relative fluorescence intensity on spectral flow cytometry. **(B)** Frequencies of CD69+, Perforin (PRF)- NK cells after co-culture. **(C)** Heatmap showing percentage of NK cells positive for various phenotypic markers after co-culture. **(A-C)** NK cells (*n*=5) were either co-cultured for 72 hours with HepaRG (Non-tumor experienced, nNK) or SNU475 (Tumor-experienced, tNK) compared to control (cNK). **(D)** Transcriptional signature of tumor-experienced NK cells (*n*=4) is associated with immune regulatory pathways. Comparative gene ontology (GO) immune processes enrichment analysis for the upregulated genes expressed ($p<0.05$, Fold change>1.5) in tumor-experienced NK cells as compared to either non tumor-experienced NK (nNK) and control (cNK). Node size is proportional to the adjusted p value for GO term enrichment. Node color is set according to the relative enrichment of the GO term in either comparison of tNK versus cNK (Red) or tNK versus nNK (Dark Blue); varying shades of purple indicates a relative proportion of genes contributing to the enriched gene sets. The leading GO terms were annotated with a larger font.

Figure 3. Tumor-experienced NK cells induce suppressive monocytes with defective antigen presentation to CD8 T cells.

(A) Percentage of HLA-DR^{high} monocytes after three days co-culture with control NK cells (cNK) or tumor-experienced NK cells (tNK) (*n*=9). Friedman test with multiple comparisons was used to test for significance. **(B)** Percentage of CD73+ monocytes after three days of co-culture with cNK cells or tNK cells. **(C)** Percentage of arginase-1 (ARG-1)+ monocytes after three days of co-culture with cNK cells or tNK cells. **(D)** Percentage of PD-L1+ monocytes after three days of co-culture with cNK cells or tNK cells. **(B to D)** Different symbol colors represent the various tumor cell lines used to generate tNK cells as shown in legend (n= 5 monocytes alone, 5 cNK and 26 tNK cells generated from 5 different cell lines). Friedman test with multiple comparisons were used to test for significance. Refer to table S4 for information of various tumor cell lines. **(E)** Representative CFSE histogram showing dividing CD8 T cells responders in the presence or absence of CD14+ myeloid suppressors induced by tNK cells. **(F)** Proliferation of CD8 T cells in the presence of differentially conditioned monocytes (*n*=5). **(G)** Relative fold change in proliferation of CD8 T cells under myeloid cell suppression by tNK-experienced monocytes and in the presence of various selective inhibitors (*n*=5). Friedman Test was performed to test for significance comparing inhibitors-treated cultures to untreated control. (Refer to table S4 for inhibitors) **(H)** Schematics illustrating the outline of antigen-presentation assay using autologous TILs and tumor cells, in the presence of cNK-, or tNK-experienced monocytes. **(I)** Percentage of IFNγ-producing TILs upon autologous tumor stimulation in the presence of allogenic antigen-primed monocytes and in the presence or absence of cNK or tNK (*n*>4 per group). Friedman test with multiple comparisons were used to test for significance. **(F, G and I)** Data represented in tukey's boxplots. ns=non-significant, *p<0.05, **p<0.01 and ***p<0.001.

Commented [DH128]: Please avoid using red and green together in figures, as readers with red-green colorblindness will be unable to interpret figures, as in Figs 3B, C, D, F, and I

Commented [NSY129R128]: Amended figures.

Commented [DH130]: Define these at first use in the figure legends

Commented [NSY131R130]: ok

Commented [DH132]: Please describe each of these panels seperately

Commented [NSY133R132]: noted

Commented [DH134]: What is this comparison to? Untreated?

Commented [NSY135R134]: Yes. Amended in legend to clarify

Figure 4. Tumor-experienced NK cells enhance the survival and proliferation of sXBP-1+ suppressive neutrophils.

(A) Experimental outline of neutrophils co-cultured with tumor-experienced NK cells (tNK) or control NK cells (cNK). **(B)** Representative FACS plot of viable neutrophils after two days co-culture with NK cells. **(C)** Percentage of viable neutrophils after 48 hours of co-culture with NK cells (*n*=8). **(D)** Representative FACS plot showing the expression of COX-2 and arginase-1 (ARG1) on CD15+ neutrophils in the presence or absence of NK cells. **(E)** Frequency of COX2+ neutrophils after 48 hours co-culture with NK cells. **(F)** Frequency of Arginase-1 (ARG1)+ neutrophils after 48 hours co-culture with NK cells. **(G)** Frequency of IFNγ-producing CD8 T cells in a suppression assay with autologous neutrophils and NK cells. **(E, F and G)** Friedman test with multiple comparisons was used to test for significance (*n*=6). **(H)** Representative histograms based on the fluorescence intensity of spliced XBP-1 (sXBP-1) expressed on CD15+ neutrophils after co-culture with NK cells for 48 hours. **(I)** Frequency of sXBP-1+ neutrophils after 48 hours of co-culture with NK cells (*n*=6). Friedman test with multiple comparisons were used to test for significance. **(J)** Normalized fold change in the expression of Ki67 on sXBP-1+ and sXBP-1- neutrophils after 48 hours of NK cell co-culture. Kruskal-Wallis test was used to test for significance (*n*=6). **(K)** Relative fold change of IFNγ-producing CD8 T cells within a suppression assay in the presence of neutrophils-NK cell co-culture pre-treated with tunicamycin. Kruskal-Wallis test was used to test for significance (*n*=7). **(C, J and K)** Data is presented in tukey's box plots. **P*<0.05, ***P*<0.01 and ****P*<0.001.

Commented [NSY136]: Redefined tNK and cNK

Commented [NSY137]: Separated description for panels E and F

Commented [DH138]: Please avoid using red and green together in figures, as readers with red-green colorblindness will be unable to interpret figures

Commented [NSY139R138]: Amended

Figure 5. Combinatorial analysis of NK cells and MDSCs within patient tumors reveals NK cell-derived IL-6 as a driver of suppressive myeloid phenotypes

(A) Frequencies of NK cells within the immune compartment of primary breast cancer tumors (n=29). **(B)** Spearman correlation matrix for the frequencies of various tumor-infiltrating immune cells within a breast cancer cohort based on flow cytometric analysis (n>17). Significant correlations were denoted with circles with black outlines ($P<0.05$). **(C)** Production of IL-6 by various immune and non-immune cell types in primary breast tumor samples ($n=17$). **(D)** Percentage of CD14+, HLA-DR^{low} MDSCs expressing S100A8/9 within tumors comparing cases with high MHCI expression to low MHCI expression classified by median. **(E)** Frequencies of IL-6 producing NK cells within tumors comparing cases with high MHCI expression to low MHCI expression classified by median. **(D and E)** Mann-Whitney test was used to test for significance (n=19 in total). **(F)** Production of different cytokines by NK cells from B16F10 tumors comparing wild type (WT) B16F10 to B2M-KO B16F10 ($n=6$ mice/group). Two-way ANOVA with multiple comparisons was used to test for significance. **(G)** Representative dot plot for M-MDSC (Ly6C+, CD11b^{high}) and PMN-MDSC (Ly6G+, CD11b^{high}) in B16F10 WT and B2M-KO tumors. **(H)** Frequencies of M-MDSC and PMN-MDSC in tumors comparing WT B16F10 to B2M-KO B16F10 ($n=5$ mice/group). **(I)** Frequencies of M-MDSC and PMN-MDSC in WT B16F10 tumors comparing mice with or without NK cell depletion (aNK1.1) treatment ($n=8$ mice/group). **(F to I)** Either WT or B2M-KO B16F10 tumor cells were injected subcutaneously into the right flank of C57BL/6 WT mice (See methods for details). **(J)** Frequencies of M-MDSC in tumors comparing RMA to RMA-S and mice with or without NK cell depletion (aNK1.1) treatment ($n>4$ mice/group). **(K)** Representative dot plot for production of IFNγ and IL-6 by NK cells within RMA and RMA-S tumors. **(L)** Frequencies of IL-6 producing NK cells within tumors comparing RMA to RMA-S ($n=4$ mice/group). Student t-test was used to test for significance

Commented [DH140]: Please avoid using red and green together in figures, as readers with red-green colorblindness will be unable to interpret figures

Commented [NSY141R140]: Amended

Commented [NSY142]: Separated descriptions of panels D and E.

Commented [DH143]: Please include some details regarding the mouse model used, mouse strain used, where tumors were inoculated

Commented [SN144R143]: Included as description for (F to I)

Commented [DH145]: Since this is a new model please describe a bit

Commented [SN146R145]: Included as description for (J to L)

between two experimental conditions. **(J to L)** Either RMA or RMA-S tumor cells were injected subcutaneously into the right flank of C57BL/6 WT mice (See methods for details). **(H to J)** One-way ANOVA with multiple comparisons was used to test for significance. *P<0.05, **P<0.01, ***P<0.001 and ****P<0.0001. **(M)** Expression of INOS, PD-L1 and Arginase-1 (ARG-1) in healthy C57BL/6 wild type mouse bone marrow-derived monocytes after 3 days co-culture with tumor-isolated NK cells from either WT MC38 or B2M-KO MC38 tumors. Percentage of positive cells were normalized to monocyte alone control group. Student t-test was used to compare cultures using WT-NK cells to those with IL-6 KO NK cells (n>3).

Commented [DH147]: Mouse?

Commented [SYN148R147]: yes. amended

Figure 6. NK cell-derived IL-6 contributes to MDSC-mediated immune suppression and tumor progression

(A) Tumor growth over 15 days post B16F10 co-inoculation with NK cells (WT NK cells, *n*=5 or IL6-KO NK cells, *n*=5) and without NK cells (Control, *n*=7). Two-way ANOVA was used to test for significance. **(B)** Final volume at day 15 post tumor inoculation. One-way ANOVA with multiple comparison was used to test for significance. **(A and B)** B16F10 tumor cells were subcutaneously injected into the right flank of C57BL/6 WT mice either alone or co-injected with WT NK cells or NK cells isolated from IL-6KO mice (See methods for details). **(C)** Representative dot plots for S100A8/9 and arginase-1 (ARG) expression in myeloid cells after co-culture with either siRNA control NK cells (siControl-NK) or IL-6 knockdown NK cells(siIL6-NK) in vitro. **(D)** Fold change expression of S100A8/9, arginase, PD-L1 and DAF-FM (nitric oxide probe) within monocytes after co-culture with either siRNA control NK cells (siControl-NK) or IL-6 knockdown NK cells (siIL6-NK). Wilcoxon signed rank test was used to test for significance for every phenotypic marker. Data presented in tukey's boxplots (*n*>5). **(E)** Percentage of dividing CD8 T cells in the presence of NK cells and myeloid cells after 48 hours of concurrent bead stimulation. Friedman test with multiple paired comparisons were used to test for significance (*n*=6). **(F)** Schematic outline of zebrafish xenografts microinjected with patient-derived cells. **(G)** Representative confocal images of zebrafish engrafted with patient-derived melanoma (magenta) and TILs (blue). Areas of nitric oxide accumulation are stained by DAF-FM (green). Scale bar denotes 150mm in length. White boxes highlight the presence of injected tumor cells in both the yolk sac and tail of the zebrafish larvae. **(H)** Number of red fluorescent-labelled tumor regions within zebrafish larvaes injecting with different immune cell types (*n*=35 zebrafish in total). **(I)** Number of green fluorescent-labelled regions (nitric oxide accumulation) within zebrafish larvaes injecting with different immune cell types (*n*=41 zebrafish in total). **(F and I)** Kruskal

Commented [DH149]: Please introduce the model again here

Commented [SN150R149]: Added for panels A and B

Commented [DH151]: Author, correct?

Commented [SYN152R151]: correct

Commented [DH153]: What are the boxes highlighting?

Commented [SN154R153]: Additional description included

Commented [DH155]: Regions or zebrafish?

Commented [SN156R155]: Zebrafish. amended

Commented [DH157]: Zebrafish or regions?

Commented [SN158R157]: Zebrafish. amended

Wallis test was used to determine significance between different experimental groups. ns = not significant, *P<0.05, **P<0.01 and ****P<0.0001.

Figure 7. Inhibition of IL6/STAT3 axis alleviates NK/MDSC-mediated immune suppression of anti-tumor responses

(A) Annotated pie chart for the proportion of phosphorylated signals expressed by monocytes after co-culture with control NK cells (cNK) cells or tumor-experienced NK cells (tNK cells) (*n*=6). **(B)** Frequency of monocytes expressing phosphorylated STAT3 (pS727) after co-culture with cNK cells or tNK cells. **(C)** Frequency of neutrophils expressing phosphorylated STAT3 (pS727) after co-culture with cNK cells or tNK cells. **(B and C)** Friedman test with multiple comparisons was used to test for significance (*n*=6). tNK cells here referred to NK cells co-cultured three days with KADA melanoma tumor cell line which were then FACS-sorted for subsequent monocyte co-culture. **(D)** Schematic illustrating experimental design for xenograft model using NSG mice. All mice were subcutaneously injected with KADA tumor cells into the right flank on day 0 and TILs together with monocytes on day 7. Mice were divided into four groups (G1-G4) where mice in groups G2 and G3 were treated with NK cells and mice in groups G2 and G4 were treated with Tocilizumab. **(E)** Representative lung sections from mice in each group with HLA-ABC^{high} tumor cells identified based on fluorescence intensity and minimum cell diameter of 15um. Scale bar denotes 1mm length. **(F)** Frequency of HLA-ABC^{high} tumor cells of total cells identified based on minimum cell diameter of 15um (*n*>8 mice per group, 3 sections per mice). **(G)** Frequency of intratumoral CD14+ human monocytes of total among live cells (n>8). **(H)** Percentage of intratumoral human monocytes expressing phosphorylated STAT3 (pSTAT3) (n>7). **(I)** Frequency of PD-L1+ intratumoral human monocytes (n>7). **(J)** Frequency of arginase-1 (ARG1)+ intratumoral human monocytes (n>7 per group). **(K)** Frequency of dividing autologous CD8 T cells in a suppression assay of CD14 human monocytes isolated from tumor xenografts (*n*>4). **(F to K)** All data is presented in tukey's box plots. One way ANOVA with multiple comparisons was used to test for significance. *P<0.05, **P<0.01, ***P<0.001 and ****P<0.0001.

Commented [DH159]: Please avoid using red and green together in figures, as readers with red-green colorblindness will be unable to interpret figures, in figs7F-K

Commented [SN160R159]: Amended

Commented [SN161]: Separated descriptions for panel B and C.

Commented [DH162]: What cell line was used? Where was this injected, you show sections of lungs in the next subfigure, is this metastatic cells or is this where cells were inoculated?

Commented [SYN163R162]: amended

Commented [NSY164]: Separated descriptions for panels G to J.

Figure 1

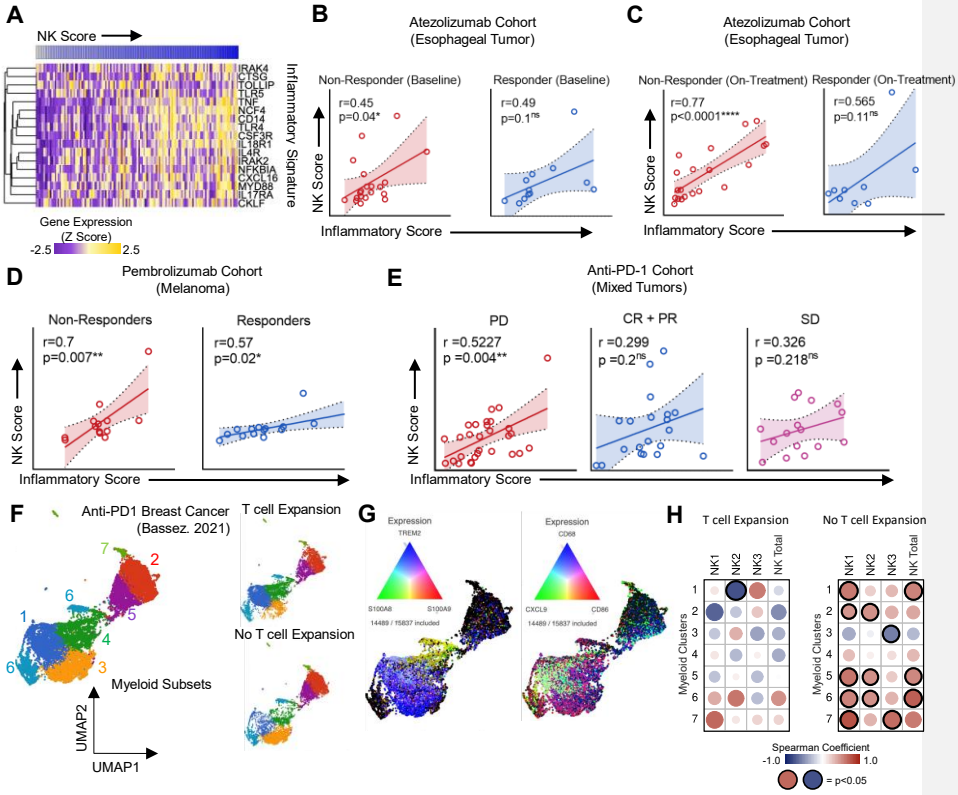
A
NK Score
Inflammatory Signature
IRAK4
ICSG
TOLLIP
TLR5
TNF
NCF4
CD14
TLR4
CSF3R
IL18R1
IL4R
IRAK2
NFKBIA
CXCL16
MYD88
IL17RA
CKLF
Gene Expression
(Z Score)
-2.5
2.5
B
Atezolizumab Cohort
(Esophageal Tumor)
Non-Responder (Baseline)
Responder (Baseline)
r=0.45
p=0.04*
r=0.49
p=0.1ns
NK Score
Inflammatory Score
C
Atezolizumab Cohort
(Esophageal Tumor)
Non-Responder (On-Treatment)
Responder (On-Treatment)
r=0.77
p<0.0001****
r=0.565
p=0.11ns
NK Score
Inflammatory Score
D
Pembrolizumab Cohort
(Melanoma)
Non-Responders
Responders
r=0.7
p=0.007**
r=0.57
p=0.02*
NK Score
Inflammatory Score
E
Anti-PD-1 Cohort
(Mixed Tumors)
PD
CR + PR
SD
r =0.5227
p =0.004**
r =0.299
p =0.2ns
r =0.326
p =0.218ns
NK Score
Inflammatory Score
F
Anti-PD1 Breast Cancer
(Bassez. 2021)
T cell Expansion
No T cell Expansion
Myeloid Subsets
UMAP2
UMAP1
G
Expression
TREM2
S100A8
S100A9
Expression
CD68
CXCL9
CD86
H
T cell Expansion
No T cell Expansion
NK1
NK2
NK3
NK Total
Myeloid Clusters
Spearman Coefficient
-1.0
1.0
= p<0.05

1270 Figure 2

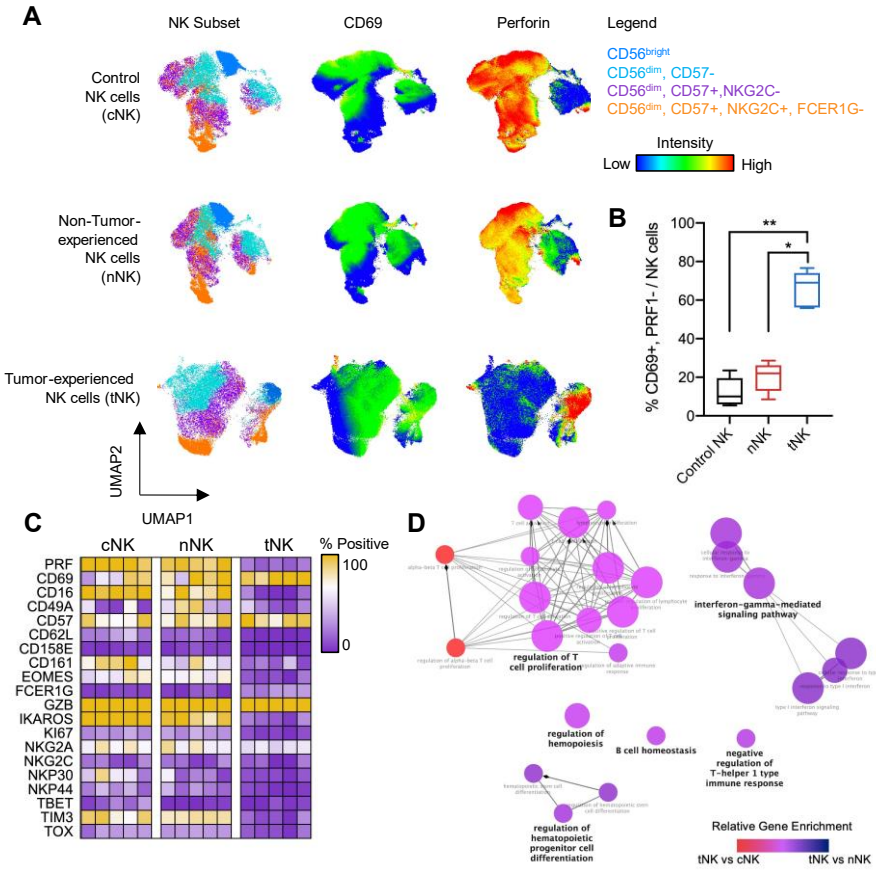

1271

1272 Figure 3

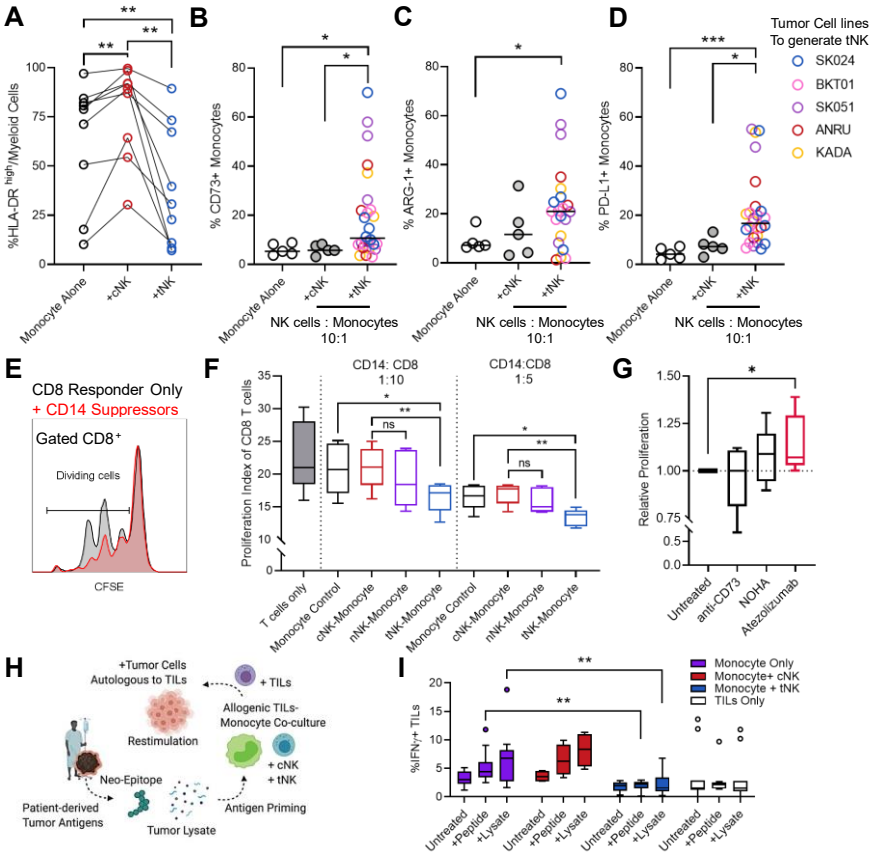

1273

1274

1275 Figure 4

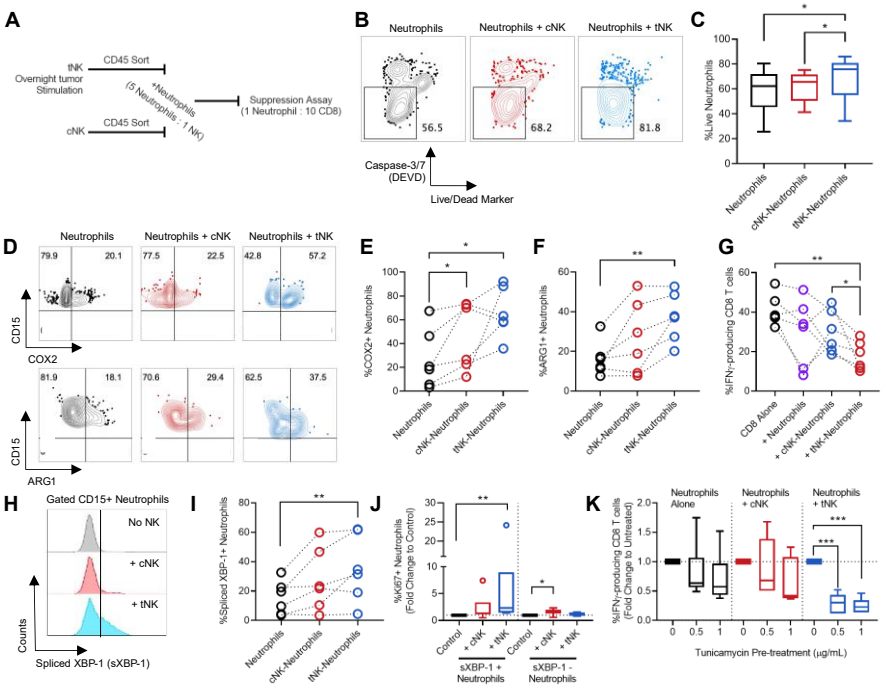

1276

Figure 5

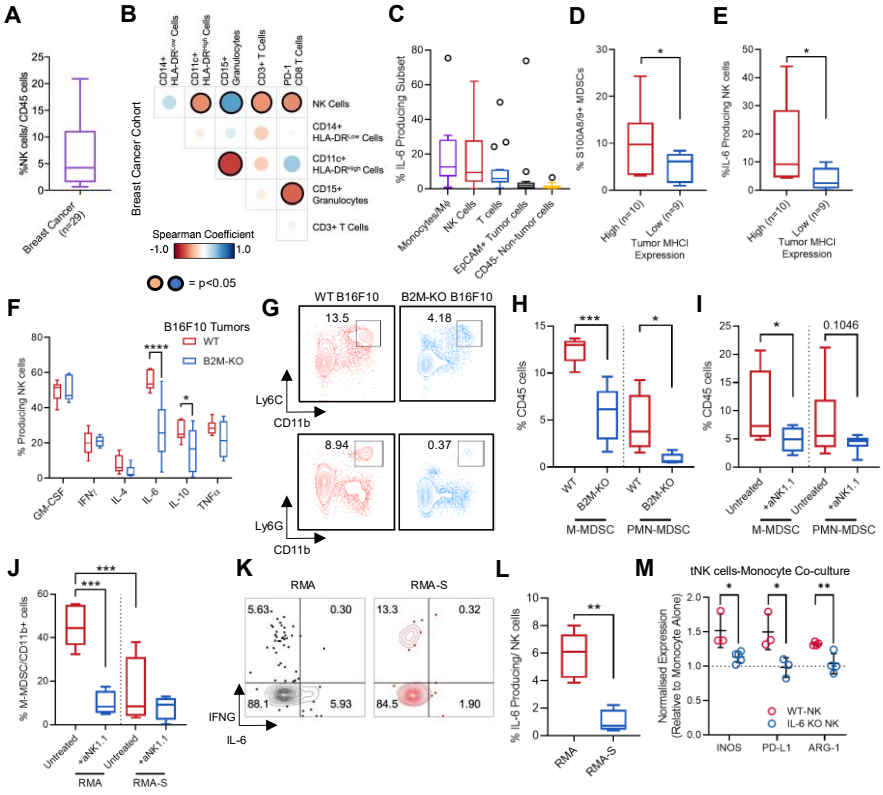
A
%NK cells/ CD45 cells
Breast Cancer (n=29)
B
Breast Cancer Cohort
CD14+ HLA-DRLow Cells
CD11c+ HLA-DRHigh Cells
CD15+ Granulocytes
CD3+ T Cells
PD-1 CD8 T Cells
NK Cells
CD14+ HLA-DRLow Cells
CD11c+ HLA-DRHigh Cells
CD15+ Granulocytes
CD3+ T Cells
Spearman Coefficient
-1.0
1.0
= p<0.05
C
% IL-6 Producing Subset
Monocytes/Mϕ
NK Cells
T cells
EpCAM+ Tumor cells
CD45- Non-tumor cells
D
% S100A8/9+ MDSCs
High (n=10)
Low (n=9)
Tumor MHCI Expression
E
%IL-6 Producing NK cells
High (n=10)
Low (n=9)
Tumor MHCI Expression
F
B16F10 Tumors
WT
B2M-KO
% Producing NK cells
GM-CSF
IFNγ
IL-4
IL-6
IL-10
TNFα
G
WT B16F10
B2M-KO B16F10
13.5
4.18
8.94
0.37
Ly6C
CD11b
Ly6G
CD11b
H
% CD45 cells
WT
B2M-KO
WT
B2M-KO
M-MDSC
PMN-MDSC
I
% CD45 cells
0.1046
Untreated
+aNK1.1
Untreated
+aNK1.1
M-MDSC
PMN-MDSC
J
% M-MDSC/CD11b+ cells
Untreated
+aNK1.1
Untreated
+aNK1.1
RMA
RMA-S
K
RMA
RMA-S
5.63
0.30
88.1
5.93
13.3
0.32
84.5
1.90
IFNG
IL-6
L
% IL-6 Producing/ NK cells
RMA
RMA-S
M
tNK cells-Monocyte Co-culture
Normalised Expression (Relative to Monocyte Alone)
WT-NK
IL-6 KO NK
INOS
PD-L1
ARG-1

Figure 6

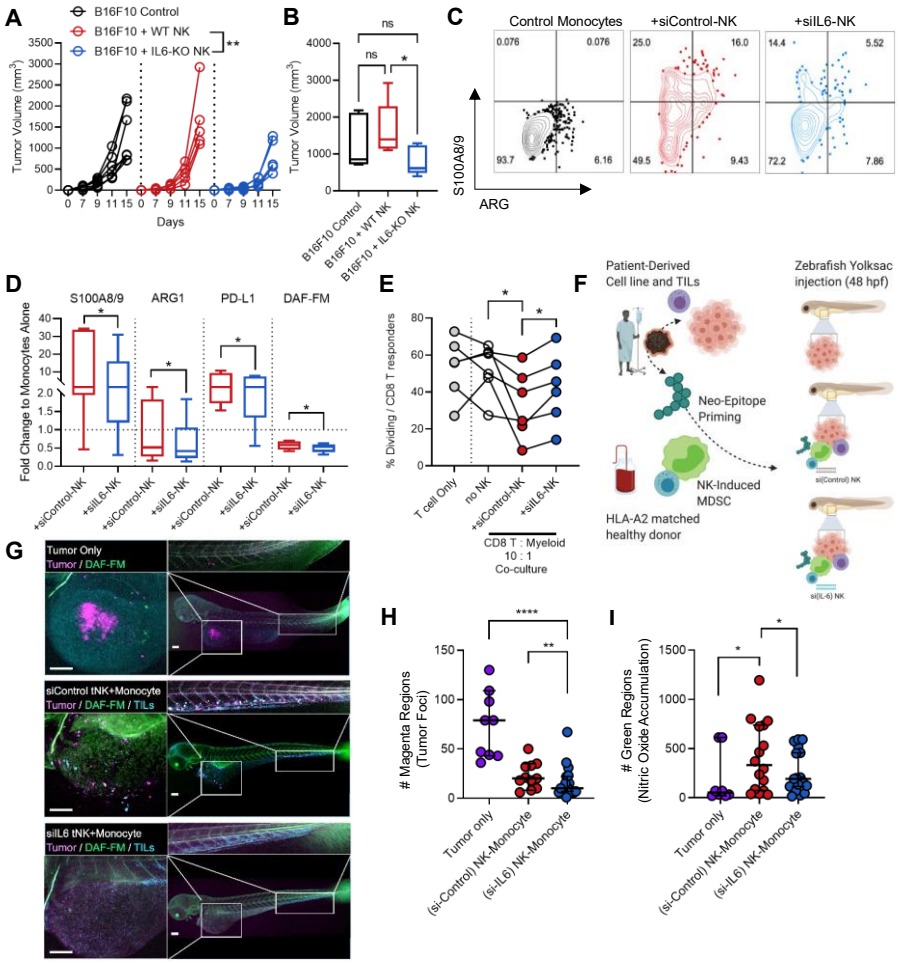
A
B16F10 Control
B16F10 + WT NK
B16F10 + IL6-KO NK
Tumor Volume (mm3)
Days
B
ns
ns
*
Tumor Volume (mm3)
B16F10 Control
B16F10 + WT NK
B16F10 + IL6-KO NK
C
Control Monocytes
+siControl-NK
+siIL6-NK
S100A8/9
ARG
0.076
0.076
93.7
6.16
25.0
16.0
49.5
9.43
14.4
5.52
72.2
7.86
D
S100A8/9
ARG1
PD-L1
DAF-FM
Fold Change to Monocytes Alone
+siControl-NK
+siIL6-NK
E
% Dividing / CD8 T responders
T cell Only
no NK
+siControl-NK
+siIL6-NK
CD8 T : Myeloid
10 : 1
Co-culture
F
Patient-Derived
Cell line and TILs
Neo-Epitope
Priming
NK-Induced
MDSC
HLA-A2 matched
healthy donor
Zebrafish Yolksac
injection (48 hpf)
si(Control) NK
si(IL-6) NK
G
Tumor Only
Tumor / DAF-FM
siControl tNK+Monocyte
Tumor / DAF-FM / TILs
siIL6 tNK+Monocyte
Tumor / DAF-FM / TILs
H
****
**
Magenta Regions
(Tumor Foci)
Tumor only
(si-Control) NK-Monocyte
(si-IL6) NK-Monocyte
I
*
*
Green Regions
(Nitric Oxide Accumulation)
Tumor only
(si-Control) NK-Monocyte
(si-IL6) NK-Monocyte

1282 Figure 7

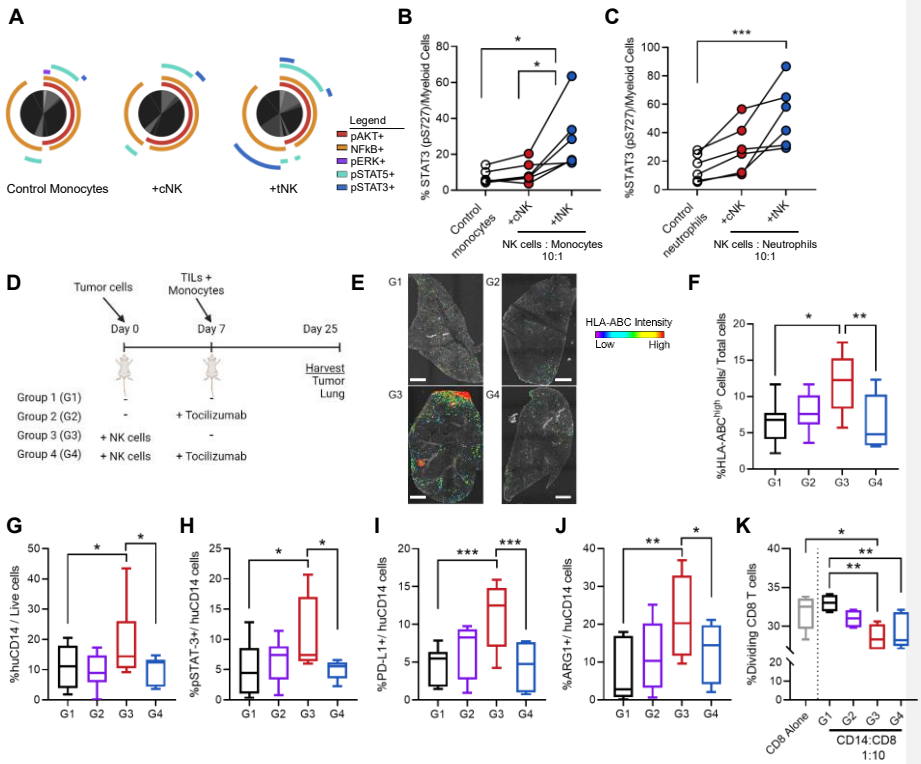

1283

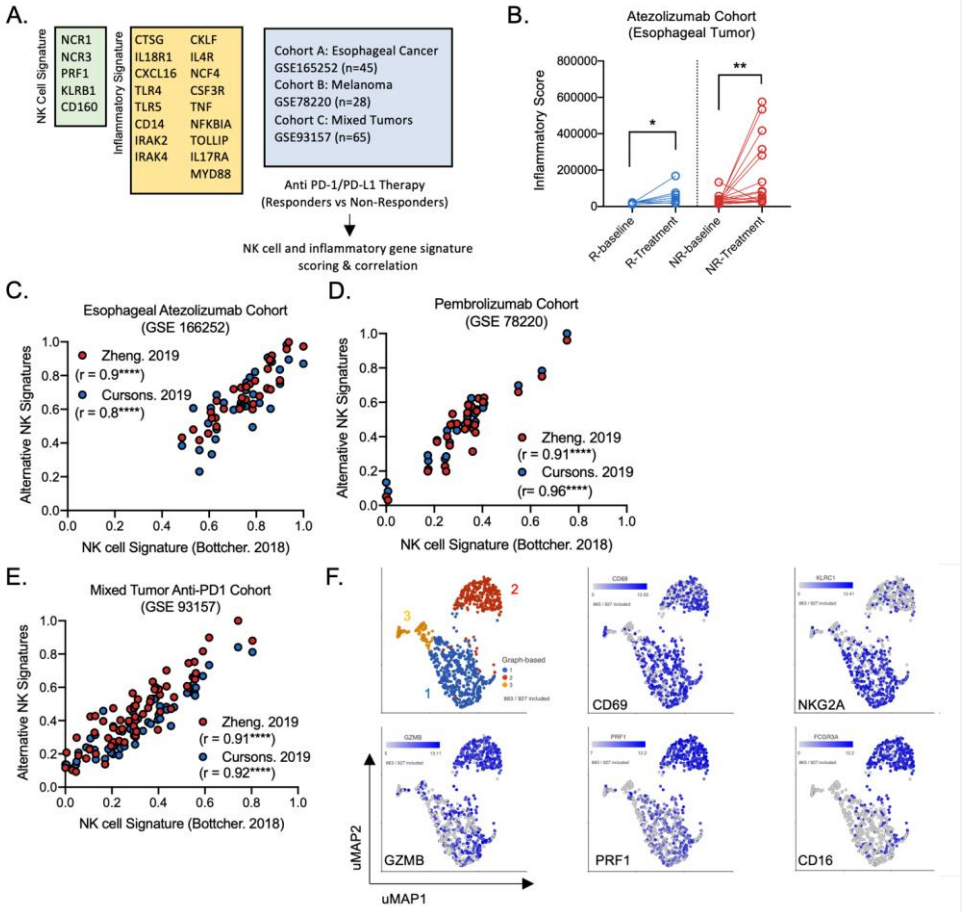

Figure S1. Co-abundance of NK cell and MDSC gene signature may not arise from increased tumor infiltration.

(A) Details of NK cell (*Bottcher et al. 2018)* and inflammatory gene signatures and the 3 cohorts used for transcriptomics analysis. **(B)** Relative inflammatory signature score comparing tumor samples collected at baseline prior to treatment and on-treatment samples within responders and non-responders in an atezolizumab esophageal tumor cohort (GSE165252, n= 24). Wilcoxon signed rank test was used for statistical testing. Correlation of ssGSEA score between NK signature *(Bottcher et al. 2018)* with 2 other alternative NK gene signatures analysed in **(C)** cohort A, **(D)** cohort B and **(E)** cohort C. (**C to E**) Pearson correlation was performed. ****P<0.0001. (F) UMAP projections of NK cell subsets grouped based on the Louvain method to reveal three clusters with normalized expression of selected NK cell genes from publicly accessed breast cancer dataset (n=29).

Commented [DH165]: Please update all titles to reflect this and remove the title in the top right corner of the figures

Commented [SN166R165]: ok

Commented [DH167]: Please make sure red and green are not used in the same figures and please note that the supplemental materials will not be top edited and will be published as is. Please make sure all nomenclature, coloring and numbering is consistent with the main text

Commented [SN168R167]: noted

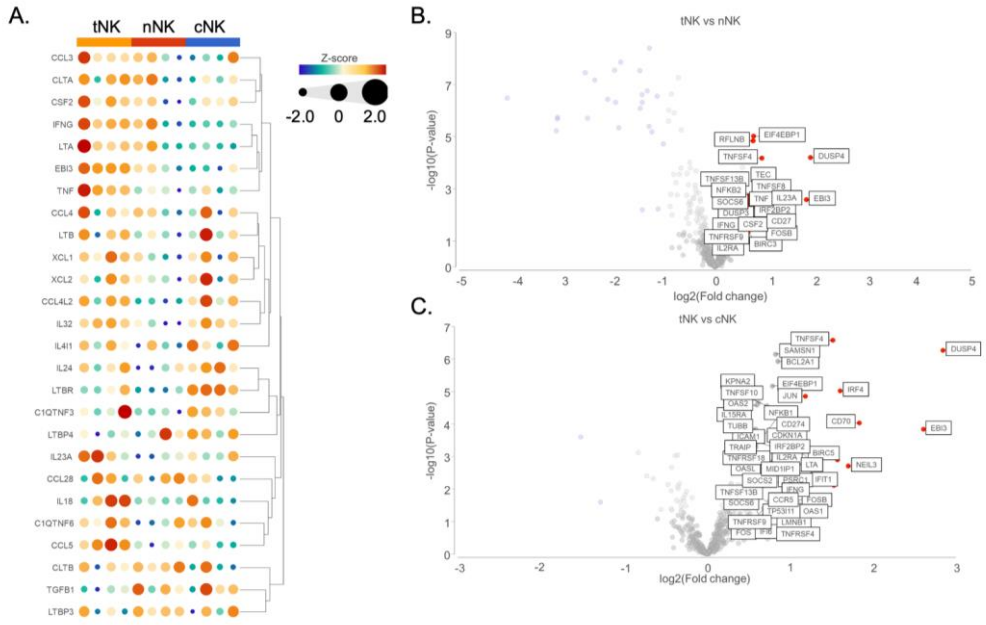

Figure S2. Differential gene expression analysis of NK cells after co-culture with tumor or non-tumor cells.

A, Hierarchical heatmap showing the normalised differential expression of inflammatory and regulatory factors in tumor-experienced NK (tNK), non-tumor-experienced NK (nNK) and control (cNK). Volcano plots showing differentially upregulated genes (with *P*-value<0.05) in **(B)** comparison of tNK versus cNK and **(C)** comparison of tNK versus nNK.

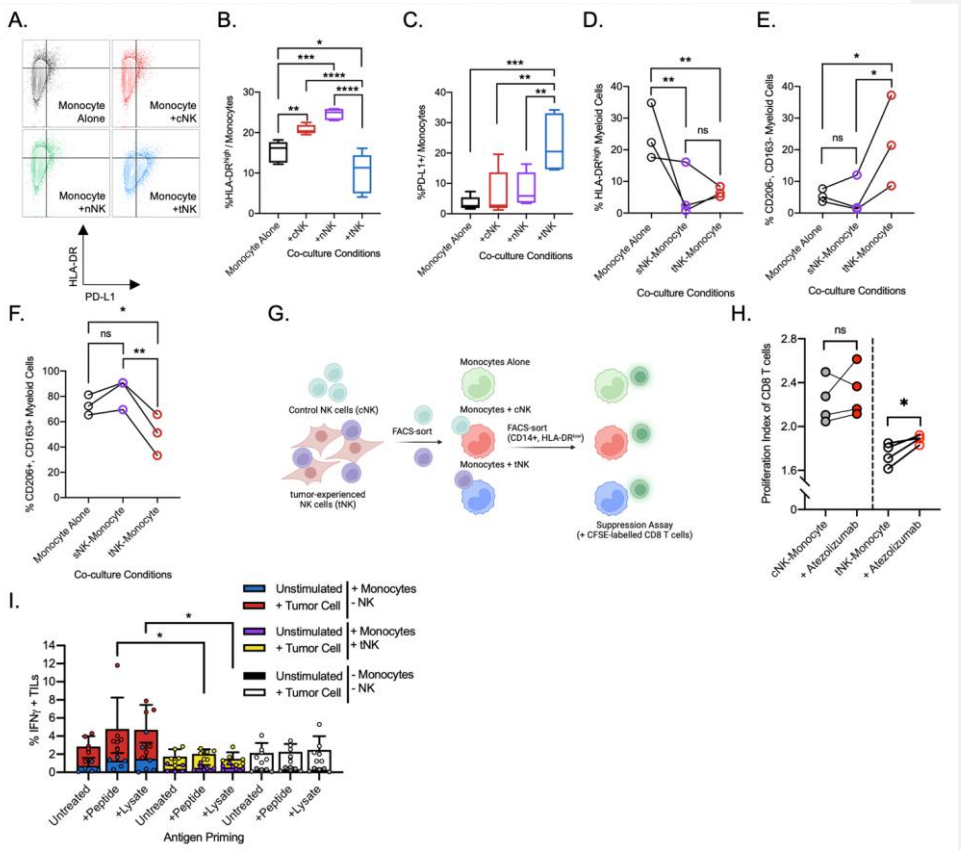

Figure S3. Tumor-experienced NK cells acquire unique immune-regulatory capacity to induce suppressive monocytes.

(A) Representative flow cytometric plots showing PD-L1 and HLA-DR expression on CD14+ monocytes after three days culture with control NK cells (cNK), non-tumor experienced NK cells (nNK) or tumor-experienced NK cells (tNK). Frequencies of **(B)** HLA-DR^{high} monocytes and **(C)** PD-L1+ monocytes after three days culture with differentially stimulated sorted NK cells (n=5). Frequencies of **(D)** HLA-DR^{high} myeloid cells, **(E)** CD206-, CD163- myeloid cells and **(F)** CD206+, CD163+ myeloid cells after co-culture with either tumor supernatant-stimulated NK cells (sNK) or tumor-experienced NK cells (tNK) after 72 hours (n=3). **(B to F)** Paired t-test was used for statistical testing. **(G)** Experimental outline of CD8 T cell suppression assay using autologous monocytes FACS-sorted based on HLA-DR expression. (**H**) Effects of atezolizumab on CD8 T cell proliferation within a suppression assay in the presence of cNK-monocytes or tNK-monocytes. Paired t-test was used to test comparisons between comparing untreated cultures and Atezolizumab (10ug/mL) treated cultures (n=4). **(I)** Percentage of IFNg-producing TILs with or without 4 hours of tumor cell restimulation in the presence of allogeneic monocytes and NK cells. Friedman test with multiple comparison was used for statistical testing.

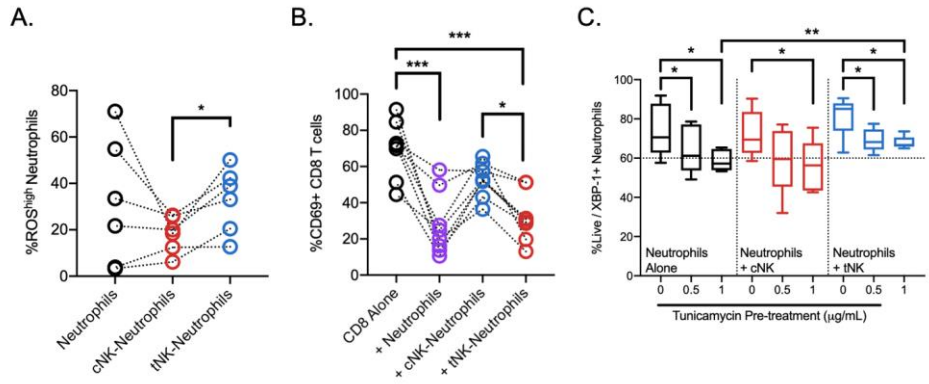

Figure S4. Tumor-experienced NK cells enhance the suppressive capacity of neutrophils.

(A) Percentage of CellROX^{high} neutrophils after 48 hours of co-culture with NK cells (n=6). **(B)** Percentage of CD69% CD8 Responder T cells in the presence of neutrophils and NK cells in a suppression assay (n=8). **(C)** Percentage of viable XBP-1+ neutrophils after 48 hours of co-culture with NK cells in the presence of increasing doses of tunicamycin (n=5). (A to C) Friedman test with multiple comparisons was used to test for statistical testing.

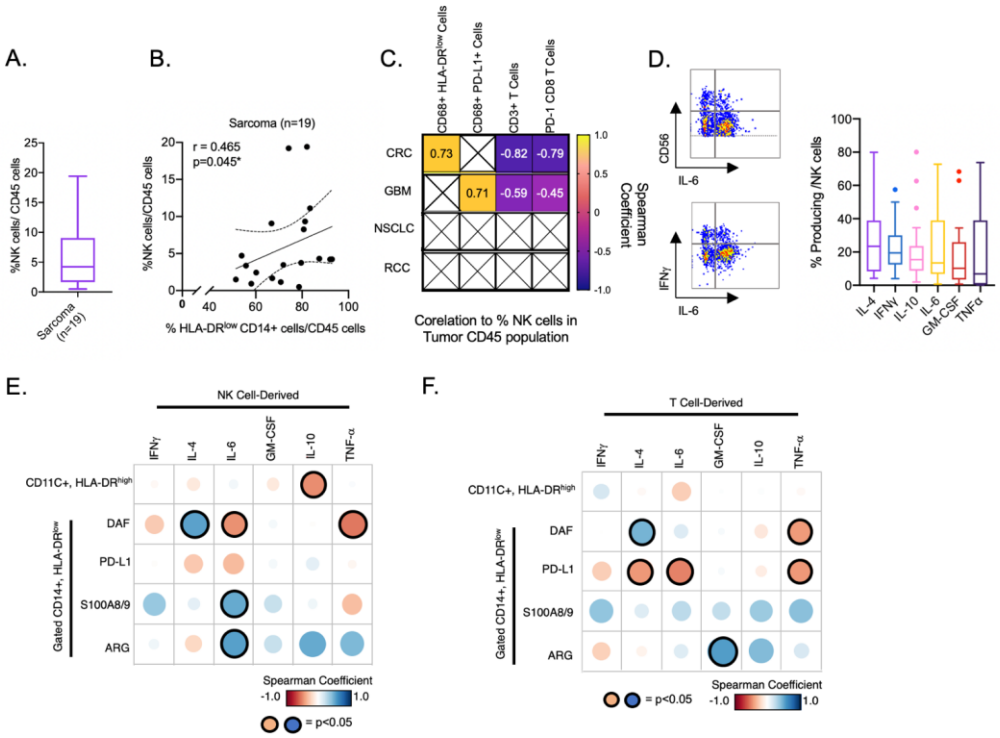

Figure S5. Positive correlation of NK cells and suppressive myeloid phenotypes in several types of solid tumors

(A) Frequencies of NK cells within the immune compartment of primary tumors from a cohort of sarcoma patients (n=19). **(B)** Spearman correlation between frequencies of NK cells and HLA-DR^{low}, CD14+ monocytes in primary tumors of the sarcoma cohort (n=19). **(C)** Correlation for NK cells, T cells and suppressive CD68+ myeloid cells in colorectal cancer (CRC), glioblastoma (GBM), non-small cell lung cancer (NSCLC) and renal clear cell carcinoma (RCC) based on a repository-accessed flow cytometry data (n>20). **(D) Left**; Representative dot plot for IL-6+ NK cells and their expression of CD56 and IFNg in patient tumors. **Right**; Frequencies of NK cells producing various cytokines measured by intracellular flow cytometry staining (n>22). Correlation matrix for the relationship between **(E)** NK cell-derived cytokines **(F),** T cell-derived cytokines and the phenotype of monocytic-MDSCs (n=18). Spearman estimates with a p-value less than 0.05 were indicated by circular symbols with black outlines.

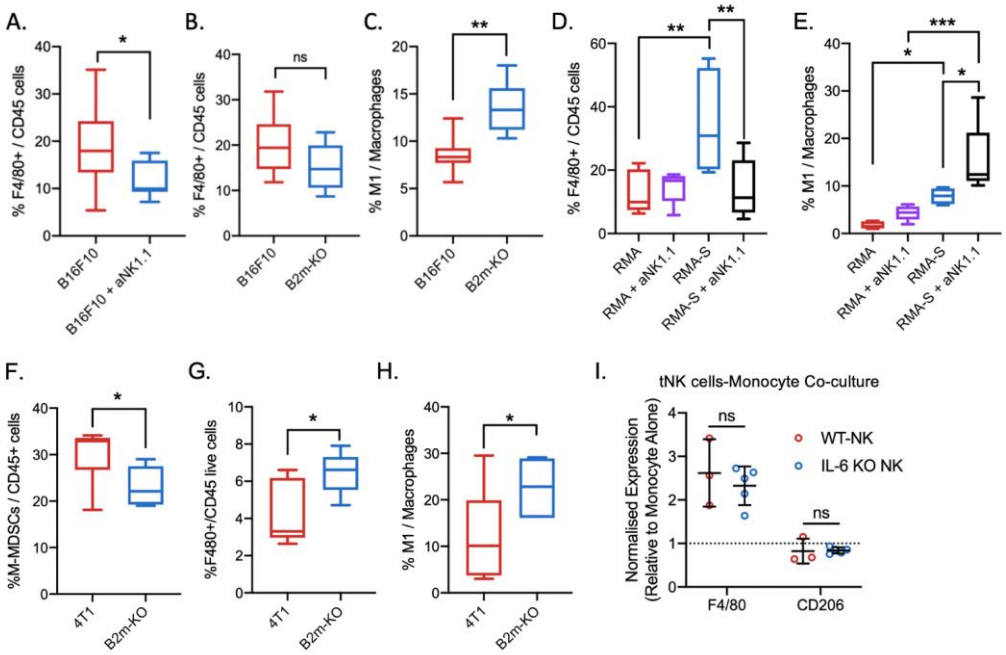

Figure S6. Tumor MHCI expression alters the proportion of M1 macrophages within the tumor microenvironment.

Frequencies of total TAMs (F4/80+ cells over total CD45+ immune cells) in comparisons of **(A)** NK cell depleted B16F10 model and **(B)** MHC-deficient (B2m-KO) tumor model. **(C)** Proportion of M1 macrophages (MHCII^{high}, CD11c+) comparing WT B16F10 tumors to B2m-KO tumors (n>6). Frequencies of **(D)** total TAMs and **(E)** M1 macrophages in comparison of RMA and RMAS tumors with or without NK cell depletion (n>4). Frequencies of **(F)** M-MDSCs and **(G)** total TAMs comparing WT 4T1 to B2m-KO 4T1 tumors (n>7). **(H)** Proportion of M1 macrophages comparing WT 4T1 to B2m-KO 4T1 tumors (n>7). **(I)** Expression F4/80 and CD206 in healthy bone marrow-derived monocytes after three days co-culture with tumor-isolated NK cells from either WT MC38 or B2M-KO MC38 tumors. Student t-test was used to compare cultures using WT-NK cells to those with IL-6 KO NK cells (n>3).

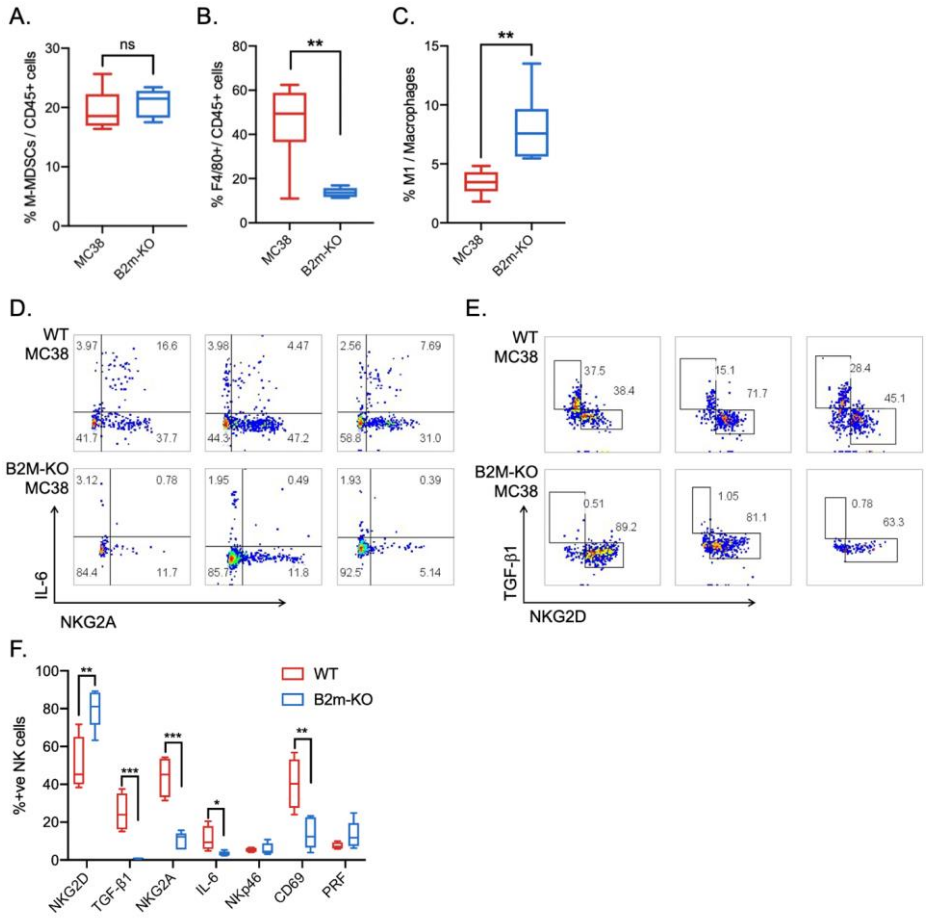

Figure S7. Differential NK cell phenotype in MC38 tumors is influenced by tumor MHCI expression.

Frequencies of **(A)** M-MDSCs and **(B)** total TAMs comparing WT MC38 to B2m-KO MC38 tumors. **(C)** Proportion of M1 macrophages comparing WT 4T1 to B2m-KO 4T1 tumors (n=6 per group). Representative dotplots for **(D)** IL-6 over NKG2A and **(E)** TGFβ1 over NKG2D expression on NK cells within WT MC38 tumors and B2m-KO MC38 tumors. **(F)** Frequencies of intratumoral NK cells expressing various phenotypic markers comparing WT (n=4) to B2m-KO MC38 tumors (n=5). **(A to F)** Paired t test was used for statistical testing.

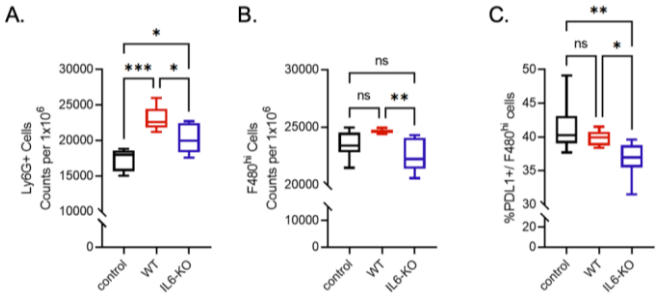

Figure S8. Altered myeloid cell frequencies within tumors with IL6-KO NK cells.

Absolute **(A)** Ly6G+, CD11b+ myeloid cells and **(B)** F480^{hi} cell counts per million live cells in B16F10 tumors (control, n=6) or with co-inoculated NK cells (WT-NK or IL6-KO NK, n=5).
(C) Percentage frequencies of PDL1+ F480^{hi} cells in B16F10 tumors (control, n=6) or with co-inoculated NK cells (WT-NK,n=8 or IL6-KO NK, n=7). **(A to C)** One-way ANOVA with multiple comparisons was used to statistical testing. (Sample size, n=6 for B16F10 control, n= 5 for B16F10+ WT NK and n=5 for B16F10+ IL6-KO NK) ns= non-significant, *P<0.05, **P<0.01 and ***P<0.001.

Commented [DH169]: Please make sure to use this word only to report statistical significance and always accompanied by a p value directly in the text. Any other uses of this word should be removed or replaced.

Commented [SN170R169]: Ok. It is used to define “ns” here

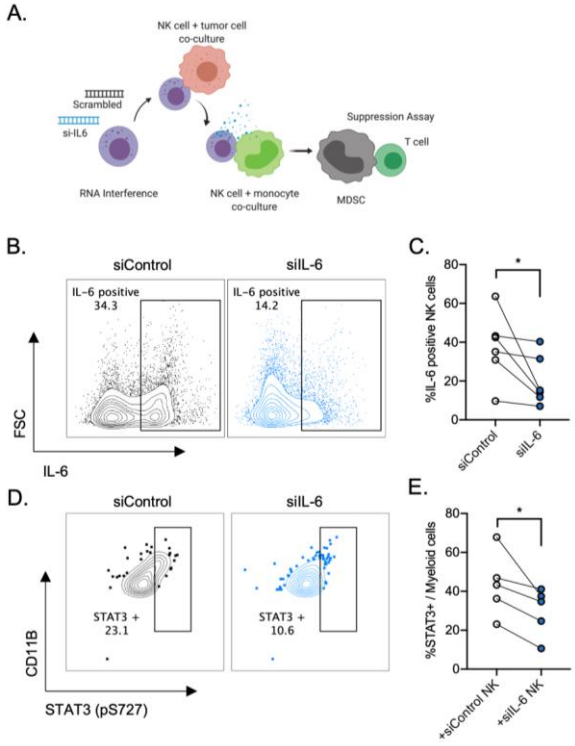

Figure S9. IL-6 derived from NK cells modulates STAT3 activity in myeloid cells.

(A) Schematic illustration of experimental outline for IL-6 knockdown in NK cells by siRNA. **(B)** Representative dotplot showing percentage of IL-6 positive NK cells 48 hours post transfection of siRNA. **(C)** Percentage of IL-6 positive NK cells 48 hours post transfection of siRNA. (n=5) **(D)** Representative dotplot showing percentage of STAT3 (pS727) positive myeloid cells after co-culture with control NK cells or si-IL6 NK cells for 72 hours. **(E)** Percentage of STAT3 positive myeloid cells after co-culture with control NK cells or si-IL6 NK cells for 72 hours. (n=6) (C and E) Wilcoxon matched pairs-signed rank was used to statistical testing. *p<0.05.

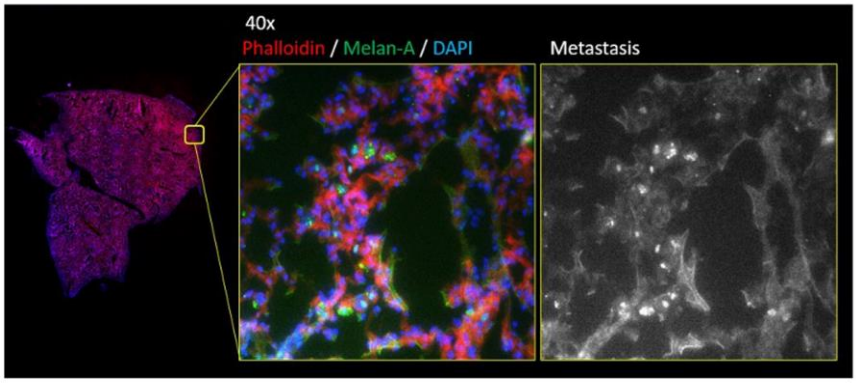

Figure S10. Expression of human Melan-A in melanoma tumor cells within lungs of NSG mice.

Table S1. List of genes used in Inflammatory gene signature

	Gene Name	Function
1	CTSG	Cathepsin G; Serine protease with trypsin- and chymotrypsin-like specificity. Cleaves complement C3. Has antibacterial activity against the Gram-negative bacterium P.aeruginosa, antibacterial activity is inhibited by LPS from P.aeruginosa, Z-Gly-Leu-Phe- CH2Cl and phenylmethylsulfonyl fluoride; Belongs to the peptidase S1 family
2	IL18R1	Interleukin-18 receptor 1; Within the IL18 receptor complex, responsible for the binding of the proinflammatory cytokine IL18, but not IL1A nor IL1B (Probable). Contributes to IL18-induced cytokine production, either independently of SLC12A3, or as a complex with SLC12A3 (By similarity); CD molecules
3	CXCL16	C-X-C motif chemokine 16; Acts as a scavenger receptor on macrophages, which specifically binds to OxLDL (oxidized low density lipoprotein), suggesting that it may be involved in pathophysiology such as atherogenesis (By similarity). Induces a strong chemotactic response. Induces calcium mobilization. Binds to CXCR6/Bonzo; Belongs to the intercrine alpha (chemokine CxC) family
4	TLR4	Toll-like receptor 4; Cooperates with LY96 and CD14 to mediate the innate immune response to bacterial lipopolysaccharide (LPS). Acts via MYD88, TIRAP and TRAF6, leading to NF-kappa-B activation, cytokine secretion and the inflammatory response. Also involved in LPS-independent inflammatory responses triggered by free fatty acids, such as palmitate, and Ni(2+). Responses triggered by Ni(2+) require non-conserved histidines and are, therefore, species-specific. Both M.tuberculosis HSP70 (dnaK) and HSP65 (groEL-2) act via this protein to stimulate NF-kappa-B expression.
5	TLR5	Toll-like receptor 5; Participates in the innate immune response to microbial agents. Mediates detection of bacterial flagellins. Acts via MYD88 and TRAF6, leading to NF-kappa-B activation, cytokine secretion and the inflammatory response.
6	CD14	Monocyte differentiation antigen CD14; Coreceptor for bacterial lipopolysaccharide. In concert with LBP, binds to monomeric lipopolysaccharide and delivers it to the LY96/TLR4 complex, thereby mediating the innate immune response to bacterial lipopolysaccharide (LPS). Acts via MyD88, TIRAP and TRAF6, leading to NF-kappa-B activation, cytokine secretion and the inflammatory response.
7	CKLF	Chemokine-like factor; May play an important role in inflammation and regeneration of skeletal muscle. Partly inhibited by interleukin 10
8	IL4R	Interleukin-4 receptor subunit alpha; Receptor for both interleukin 4 and interleukin 13. Couples to the JAK1/2/3-STAT6 pathway. The IL4 response is involved in promoting Th2 differentiation. The IL4/IL13 responses are involved in regulating IgE production and, chemokine and mucus production at sites of allergic inflammation. In certain cell types, can signal through activation of insulin receptor substrates, IRS1/IRS2
9	NCF4	Neutrophil cytosol factor 4; Component of the NADPH-oxidase, a multicomponent enzyme system responsible for the oxidative burst in which electrons are transported from NADPH to molecular oxygen, generating reactive oxidant intermediates. It may be important for the assembly and/or activation of the NADPH-oxidase complex
10	CSF3R	Granulocyte colony-stimulating factor receptor; Receptor for granulocyte colony-stimulating factor (CSF3), essential for granulocytic maturation. Plays a crucial role in the proliferation, differientation and survival of cells along the neutrophilic lineage. In addition it may function in some adhesion or recognition events at the cell surface; CD molecules

11	TNF	Tumor necrosis factor; Cytokine that binds to TNFRSF1A/TNFR1 and TNFRSF1B/TNFBR. It is mainly secreted by macrophages and can induce cell death of certain tumor cell lines. It is potent pyrogen causing fever by direct action or by stimulation of interleukin-1 secretion and is implicated in the induction of cachexia, Under certain conditions it can stimulate cell proliferation and induce cell differentiation. Impairs regulatory T-cells (Treg) function in individuals with rheumatoid arthritis via FOXP3 dephosphorylation.
12	NFKBIA	NF-kappa-B inhibitor alpha; Inhibits the activity of dimeric NF-kappa-B/REL complexes by trapping REL dimers in the cytoplasm through masking of their nuclear localization signals. On cellular stimulation by immune and proinflammatory responses, becomes phosphorylated promoting ubiquitination and degradation, enabling the dimeric RELA to translocate to the nucleus and activate transcription.
13	TOLLIP	Toll-interacting protein; Component of the signaling pathway of IL-1 and Toll-like receptors. Inhibits cell activation by microbial products. Recruits IRAK1 to the IL-1 receptor complex. Inhibits IRAK1 phosphorylation and kinase activity. Connects the ubiquitin pathway to autophagy by functioning as a ubiquitin- ATG8 family adapter and thus mediating autophagic clearance of ubiquitin conjugates. The TOLLIP-dependent selective autophagy pathway plays an important role in clearance of cytotoxic polyQ proteins aggregates.
14	IL17RA	Interleukin-17 receptor A; Receptor for IL17A. Receptor for IL17F. Binds to IL17A with higher affinity than to IL17F. Binds IL17A and IL17F homodimers as part of a heterodimeric complex with IL17RC. Also binds heterodimers formed by IL17A and IL17F as part of a heterodimeric complex with IL17RC. Receptor for IL17C as part of a heterodimeric complex with IL17RE. Activation of IL17RA leads to induction of expression of inflammatory chemokines and cytokines such as CXCL1, CXCL8/IL8 and IL6; CD molecules
15	IRAK2	Interleukin-1 receptor-associated kinase-like 2; Binds to the IL-1 type I receptor following IL-1 engagement, triggering intracellular signaling cascades leading to transcriptional up-regulation and mRNA stabilization.
16	MYD88	Myeloid differentiation primary response protein MyD88; Adapter protein involved in the Toll-like receptor and IL-1 receptor signaling pathway in the innate immune response. Acts via IRAK1, IRAK2, IRF7 and TRAF6, leading to NF-kappa-B activation, cytokine secretion and the inflammatory response. Increases IL-8 transcription. Involved in IL-18-mediated signaling pathway. Activates IRF1 resulting in its rapid migration into the nucleus to mediate an efficient induction of IFN-beta, NOS2/INOS, and IL12A genes.
17	IRAK4	Interleukin-1 receptor-associated kinase 4; Serine/threonine-protein kinase that plays a critical role in initiating innate immune response against foreign pathogens. Involved in Toll-like receptor (TLR) and IL-1R signaling pathways. Is rapidly recruited by MYD88 to the receptor-signaling complex upon TLR activation to form the Myddosome together with IRAK2.

1418

Table S2. Characteristics of breast cancer patient cohort

	%ER	%PR	%Ki67	Her2 status	NHG[a]	Tumor_size (mm)	Age	Nodes Status
1	0	0	75	NEG	3	40	69	NA
2	99	30	28	NEG	3	24	72	POS
3	20	0	90	NEG	3	27	89	POS
4	0	0	80	NEG	3	68	82	POS
5	0	0	90	NEG	3	50	89	NA
6	99	0	7	NEG	2	37	56	NEG
7	95	90	21	NEG	2	70	72	POS
8	90	80	61	POS	3	21	84	NEG
9	0	0	70	NEG	3	19	90	NEG
10	99	0	32	NEG	2	23	81	NEG
11	99	15	53	NEG	2	16	60	POS
12	85	5	21	NEG	2	27	73	POS
13	99	99	25	NEG	3	23	51	NEG
14	0	0	38	NEG	2	23	81	POS
15	30	0	95	NEG	3	33	74	POS
16	100	100	32	NEG	3	15	52	NEG
17	95	25	62	NEG	3	34	81	NEG
18	0	0	89	NEG	3	17	78	NEG
19	0	0	41	NEG	3	29	96	YES
20	95	5	68	NEG	3	16	53	NEG
21	100	100	23	NEG	2	16	56	NEG
22	80	3	39	NEG	3	27	41	NEG
23	99	99	38	NEG	3	16	68	NEG
24	100	0	9	NEG	2	29	76	NEG
25	75	0	15	POS	2	16	71	NEG
26	95	0	55	POS	3	33	78	NEG
27	0	0	85	NEG	3	35	41	NEG
28	100	60	24	NEG	2	19	78	POS
29	0	0	78	NEG	3	90	85	POS

[a]NHG, Nottingham histological grade. NA, Information not available.

Table S3. Characteristics of sarcoma patient cohort.

	Subtype	Tumor	Size (cm)	Localisation	Mitosis/10 hpf	Margins	Age
1	Small blue round cell (Ewing-like)	Primary	7	Left thigh	60	Wide	54
2	Dedifferentiated liposarcoma, G2	Recurrent	8	Retroperitoneum	NA	Marginal	77
3	High grade chondrosarcoma, partly dedifferentiated	Recurrent	5	pelvis	NA	Wide	60
4	Sarcoma of bone, unclear subtype	Recurrent	7	Sacrum	<10	Intralesional	51
5	Leiomyosarcoma, G3	Primary	7	Right thigh	>20	Marginal	61
6	Pleomorphic leiomyosarcoma, grade 3	Primary	4	Left breast	>20	Wide	79
7	Angiosarcoma, Grade 3	Metastasis	12	Uterus	10	Marginal	NA
8	Myxofibrosarcoma, G1	Metastasis	7,7	Right inguinal	<1	Intralesional	84
9	Liposarcoma, G1	Metastasis	27	Retroperitoneum	NA	Marginal	55
10	Solitary xanthogranuloma (benign)	Metastasis	3	Left arm	NA	NA	2
11	Leiomyosarcoma, G1	Metastasis	3,5	Right thigh	<10	Wide	68
12	Pleomorphic liposarcoma, G3	Metastasis	11	Abdominal wall	>20	Intralesional	93
13	Undifferentiated	Recurrent	7	Abdominal wall	>20	Marginal	64
14	BCOR-sarcoma	Primary	18	Left femur	NA	Intralesional	18
15	Leiomyosarcoma, G3	Primary	26	Retroperitoneum	>20	Marginal	78
16	Dedifferentiated liposarcoma	Primary	15	Abdominal	<10	Intralesional	62
17	Chondrosarcoma	Metastasis	4	Right lung	NA	Marginal	34
18	Dedifferentiated liposarcoma, G3	Primary	18	Mediastinal	>20	Intralesional	79
19	Solitary fibrous tumor	Primary	4,2	Bladder	5	Marginal	55
20	Malignant Peripheral Nerve Sheath Tumor	Recurrent	12	Left thigh	>20	Wide	42
21	Myxofibrosarcoma, G3	Primary	6,5	Right thigh	>20	Marginal	81

NA, Information not available.

Table S4. List of tumor cell lines

Cell line	Tissue Origin	Description	Species
HepaRG	Liver	Commercial bipotent hepatic progenitor cell	Human
SNU475	Liver	Commercial HCC Cell line	Human
HUH7	Liver	Commercial HCC Cell line	Human
SK024	Thigh	Established sarcoma (MPNST) cell line	Human
BKT01	Breast	Established primary breast cancer cell line	Human
SK051	Thigh	Established primary melanoma cell line	Human
ANRU	Skin	Established primary melanoma cell line	Human
KADA	Skin	Established primary melanoma cell line	Human
SK-OV-3	Ovary	Commercial ovarian adenocarcinoma	Human
B16F10	Skin	Commercial melanoma cell line	Murine
MC38	Colon	Commercial colon adenocarcinoma cell line	Murine
4T1	Breast	Commercial TNBC cell line	Murine
RMA	Hematopoietic	Established lymphoma cell line	Murine
RMA/S	Hematopoietic	Established lymphoma cell line (MHCI deficient variant)	Murine

HCC: Hepatocellular carcinoma, MPNST: Malignant Peripheral Nerve Sheath Tumor, TNBC: Triple Negative Breast Cancer

Table S5. List of Inhibitors

Reagent	Effect	Company	Catalog number
Atezolizumab (Anti-PD-L1)	Neutralisation	Selleck	A2004
Anti-CD73 Clone 7G2	Neutralisation	Thermo Fisher Scientific	41-0200
NOHA	Arginase inhibitor	Sigma	399275
Anti-IL10	Neutralisation	Biolegend	501401
Tocilizumab	IL-6R Inhibitor	Selleck	A2012
Tunicamycin	ER Stress Inducer	Sigma	T7765

1487Table S6. List of human flow cytometry antibodies and probes
1488

S/N	MARKERS	CONJUGATE	CATALOG NUMBER	COMPANY	REMARKS
1	AKT (pS473)	PE-CF594	562465	BD BIOSCIENCES	
2	ARGINASE	PACIFIC BLUE	48-3697-82	EBIOSCIENCES	
3	CD11B	APC-CY7	557754	BD BIOSCIENCES	
4	CD11C	PE-CY7	561356	BD BIOSCIENCES	
5	CD14	BV785	563698	BD BIOSCIENCES	
6	CD15	PerCP-cy5.5	560828	BD BIOSCIENCES	
7	CD3	BV650	563852	BD BIOSCIENCES	
8	CD3	PE-CY5	15-0038-42	EBIOSCIENCES	
9	CD45	BV650	304044	BIOLEGEND	
10	CD45	PERCP-EFLUOR 710	46-0459-42	EBIOSCIENCES	
11	CD56	BV570	318330	BIOLEGEND	
12	CD68	PE-CF594	564944	BD BIOSCIENCES	
13	CD69	BV785	310931	BIOLEGEND	
14	CD8	PE-CY7	25-0088-42	EBIOSCIENCES	
15	CellROX Deep Red	APC	C10422	THERMO FISHER	ROS Stain
16	DAF-FM	FITC	D23844	THERMO FISHER	Nitric Oxide stain
17	DR-5	PE	307406	BIOLEGEND	
18	EPCAM	BV711	324239	BIOLEGEND	
19	ERK1/2 Phospho (Thr202/Thy204)	PE-CY7	369516	BIOLEGEND	
20	FIXABLE LIVE/DEAD	AMCYAN	L34957	THERMO FISHER	Dead cell marker
21	FIXABLE LIVE/DEAD	APC-CY7	L34975	THERMO FISHER	Dead cell marker
22	GM-CSF	BIOTIN	130-105-760	MILTENYI	assay kit
23	HLA-ABC	FITC	560965	BD BIOSCIENCES	
24	HLA-DR	BV650	564231	BD BIOSCIENCES	
25	IFNY	PE	130-054-201	MILTENYI	assay kit
26	IL-10	APC	130-090-435	MILTENYI	assay kit
27	IL-4	PerCP-cy5.5	500821	BIOLEGEND	
28	IL-6	PE-CY7	501119	BIOLEGEND	
29	LOX-1	PACIFIC BLUE	358609	BIOLEGEND	

30	NFKB p65 (pS529)	BV421	565446	BD BIOSCIENCES	
31	NKP46	PACIFIC BLUE	562099	BD BIOSCIENCES	
32	PD-L1	BV785	329736	BIOLEGEND	
33	PD1	APC	17-9969-41	EBIOSCIENCES	
34	PERFORIN	PE	308106	BIOLEGEND	
35	S100A8/9	ALEXA FLUOR 647	566010	BD BIOSCIENCES	
36	STAT3 (PS727)	ALEXA FLUOR 488	558085	BD BIOSCIENCES	
37	STAT5 (PY694)	ALEXA FLUOR 647	561320	BD BIOSCIENCES	
38	STREPTAVIDIN	FITC	554060	BD BIOSCIENCES	
39	TNFA	BV785	502948	BIOLEGEND	
40	XBP1	ALEXA FLUOR 647	647506	BIOLEGEND	

1489
1490

1491Table S7. List of mouse flow cytometry antibodies and probes
1492

1	FIXABLE LIVE/DEAD	AMCYAN	L34957	THERMO FISHER SCIENTIFIC	Dead cell marker
2	FIXABLE LIVE/DEAD	APC-CY7	L34975	THERMO FISHER SCIENTIFIC	Dead cell marker
3	CD11B	PE-CY7	25-0112-82	EBIOSCIENCES	
4	LY6G	PACIFIC BLUE	560603	BD BIOSCIENCES	
5	LY6C	PE	128007	BIOLEGEND	
6	CD3	PE/Fire700	100272	BIOLEGEND	
7	CD45	ALEXA FLUOR 700	103128	BIOLEGEND	
8	IFNY	BV785	505837	BIOLEGEND	
9	H2Kb	BV421	116525	BIOLEGEND	
10	IL-4	PERCP/CY5.5	504123	BIOLEGEND	
11	IL-6	APC	504507	BIOLEGEND	
12	IL-10	PE-DAZZLE 594	505033	BIOLEGEND	
13	GM-CSF	PE-CY7	505411	BIOLEGEND	
14	TNF-A	BV605	506329	BIOLEGEND	
15	NK1.1	BV421	108741	BIOLEGEND	

1493

Table S8. Human NK cell panel for spectral flow cytometry

S/N	MARKER	CONJUGATE	CATALOG #	SUPPLIER
1	LIVE DEAD BLUE	BUV496	L23105	THERMO FISHER
2	CD62L (L-SELECTIN)	APC-FIRE 810	304866	BIOLEGEND
3	CD19	BUV661	741604	BD BIOSCIENCES
4	CD158E	R718	567046	BD BIOSCIENCES
5	CD3	BUV661	612964	BD BIOSCIENCES
6	CD14	BUV661	741603	BD BIOSCIENCES
7	CD159A (NKG2A)	PE-CY7	B10246	BECKMAN COULTER
8	CD336 (NKP44)	APC	325110	BIOLEGEND
9	CD57	EFLUOR 450	48-0577-42	THERMO FISHER
10	CD49A	APC-FIRE 750	328318	BIOLEGEND
11	FCER1G	FITC	FCABS400F	MERCK
12	CD16	BV570	302036	BIOLEGEND
13	CD159C (NKG2C)	BB700	748162	BD BIOSCIENCES
14	CD337 (NKP30)	BV605	325234	BIOLEGEND
15	CD56	BV650	318344	BIOLEGEND
16	CD161	BV785	339930	BIOLEGEND
17	CD69	BUV563	748764	BD BIOSCIENCES
18	CD366 (TIM3)	BUV737	568680	BD BIOSCIENCES
19	CD45	BUV805	612891	BD BIOSCIENCES
20	PERFORIN	BV510	308120	BIOLEGEND
21	GRANZYME B	BB790	563389	BD BIOSCIENCES
22	IKAROS	BV421	564865	BD BIOSCIENCES
23	T-BET	BV711	644820	BIOLEGEND
24	KI-67	BUV395	564071	BD BIOSCIENCES
25	EOMES	PE-CY5.5	35-4877-42	THERMO FISHER
26	TOX	EFLUOR 660	50-6502-82	THERMO FISHER